



Defence Research and
Development Canada

Recherche et développement
pour la défense Canada



Morphological Processing of Complex Signals

An Extension of Mathematical Morphology to AC Signals

Jean-F. Rivest

Defence R&D Canada – Ottawa

TECHNICAL REPORT

DRDC Ottawa TR 2006-004

January 2006

Canada

Morphological Processing of Complex Signals

An Extension of Mathematical Morphology to AC Signals

Jean-F. Rivest

Defence R&D Canada – Ottawa

Technical Report

DRDC Ottawa TR 2006-004

January 2006

Author

Original signed by Jean-F. Rivest

Jean-F. Rivest

Approved by

Original signed by Jean-F. Rivest

Jean-F. Rivest
Head/REW

Approved for release by

Original signed by Bert Bridgewater

Bert Bridgewater
Chair/Document Review Panel

© Her Majesty the Queen as represented by the Minister of National Defence, 2006

© Sa Majesté la Reine, représentée par le ministre de la Défense nationale, 2006

Abstract

This report presents an extension of Mathematical Morphology to complex signals. This extension is done by modifying the order relationship upon which all the morphological operators are based. This extension of Mathematical Morphology is essential if one wishes to use the methods of MM to process complex signals, such as communication and radar signals that feature an in-phase and an in-quadrature component.

All the basic operators such as dilations, erosions, openings and closings are developed in this report. The concept of geodesy on complex signals is explored in detail, along with the morphological approach to segmentation. The complex watershed transformation is also developed. These transformations are illustrated on complex test signals, radar signals, Fast Fourier Transforms and complex spectrograms.

Because of the proposed order relationship, the umbra of a complex signal is radically different from the umbra of a gray-tone function. Therefore, the implementation of measurements is also different from the classical measurements performed on gray-tone images. This is illustrated with an example: granulometry and pattern spectrum on a chirped radar signal.

Résumé

Ce rapport présente une extension de la morphologie mathématique aux signaux complexes. Cette extension est faite en modifiant la relation d'ordre totale sur laquelle tous les opérateurs morphologiques sont basés. Cette extension de la morphologie mathématique est essentielle si on souhaite utiliser les méthodes de la morphologie mathématique pour traiter de signaux complexes tels que des signaux de communication et des signaux radar qui comportent une composante en phase et une composante en quadrature de phase.

Tous les opérateurs de base tels que les dilatations, érosions, ouvertures et fermetures sont développés dans ce rapport. Le concept de géodésie sur les signaux complexes est exploré en détail, ainsi que l'approche morphologique de la segmentation. La ligne de partage des eaux complexe est également développée. Ces transformations sont illustrées sur des signaux complexes simulés, sur des signaux radars ainsi que sur des transformées de Fourier rapides et des spectrogrammes complexes.

La nouvelle relation d'ordre présentée dans ce travail implique que l'ombre d'un signal complexe est radicalement différente de l'ombre d'une fonction à niveaux de gris. Par conséquent, la mise en oeuvre de mesures sur des signaux complexes est également différente des mesures classiques calculées sur des images à niveaux de gris. Ceci est illustré par un exemple: la granulométrie et le spectre de patron d'un signal radar comprenant une dérive en fréquence.

Executive summary

Morphological Processing of Complex Signals

Jean-F. Rivest; DRDC Ottawa TR 2006-004; Defence R&D Canada – Ottawa; January 2006.

Mathematical Morphology (MM) is an image processing methodology which has been very successful in processing binary and gray-tone images. It is also applicable to 1-D signals. However, it lacks a strong conceptual framework in processing complex signals and images. The goal of this report is to provide such a framework, thus extending mathematical morphology to complex signals.

This report presents an extension of Mathematical Morphology to complex signals. This extension is done by modifying the order relationship upon which all the morphological operators are based. The proposed order relationship has been devised for AC (Alternating Current) signals, that is, signals that are mainly characterized by their amplitude and phase, which is fundamentally different from gray-tone functions. This extension of Mathematical Morphology is essential if one wishes to use the methods of MM to process complex signals, such as communication and radar signals that feature an in-phase and an in-quadrature component.

The extension of Mathematical Morphology is carried out and this report presents all the main transformations applied to complex signals, such as dilations, erosions, openings and closings. The application of complex morphological operators to real AC signals is also explored. Morphological operations that use arithmetic operators are also presented, such as morphological gradients and top-hats. This extension has proven to be sufficiently robust to include and re-define the concept of geodesy. Geodesic dilations and erosions are presented, along with reconstructions and openings by reconstruction. Geodesy plays a fundamental role in the morphological approach to segmentation. The main tool used for this approach is the watershed transformation. This report also illustrates the extension of this transformation to complex time-frequency representations such as the spectrogram.

Because of this new order relationship, the umbra of a complex signal is radically different from the umbra of a gray-tone function. Therefore, the implementation of measurements is also different from the classical measurements performed on gray-tone images. The Lebesgue measure of the umbra, it turns out, is the same as the energy of a signal. This report illustrates this result by creating a new type of granulometry, which is the morphological equivalent of spectral analysis, on complex signals.

This page intentionally left blank.

Sommaire

Morphological Processing of Complex Signals

Jean-F. Rivest; DRDC Ottawa TR 2006-004; R & D pour la défense Canada Ottawa; janvier 2006.

Ce rapport présente une extension de la morphologie mathématique (MM) aux signaux complexes. Cette extension a été faite en modifiant la relation d'ordre total sur laquelle tous les opérateurs morphologiques sont basés. La relation d'ordre proposée a été inventée pour des signaux à courant alternatif (AC), c'est-à-dire, des signaux qui sont principalement caractérisés par leur amplitude et leur phase, ce qui est fondamentalement différent des fonctions à niveaux de gris. Cette extension de la morphologie mathématique est essentielle si l'on veut utiliser les méthodes de la MM pour traiter des signaux complexes, tels que des signaux de communication et des signaux radars qui présentent une composante en phase et une autre en quadrature de phase.

L'extension de la morphologie mathématique est faite et ce rapport présente toutes les principales transformations appliquées à des signaux complexes, telles que les dilations, érosions, ouvertures et fermetures. L'application d'opérateurs morphologiques complexes sur des signaux réels AC est également présentée. Les opérations morphologiques qui utilise des opérateurs arithmétiques sont également présentées, tels les gradients morphologiques ainsi que les chapeaux haut-de-forme. Cette extension s'est avérée suffisamment robuste pour inclure et redéfinir le concept de géodésie. La dilatation et l'érosion géodésique sont présentées, ainsi que les reconstructions et les ouvertures par reconstruction. La géodésie joue un rôle fondamental dans l'approche morphologique de la segmentation. L'outil principal utilisé pour cette approche est la ligne de partage des eaux. Ce rapport illustre également l'extension de cette transformation à des représentations temps-fréquence complexes telles le spectrogramme.

A cause de cette nouvelle relation d'ordre, l'ombre d'un signal complexe est radicalement différente de l'ombre d'une fonction à teintes de gris. En conséquence, la mise en oeuvre de mesures est également différente des mesures classiques faites sur des images à niveaux de gris. Dans ce contexte, il appert que la mesure de Lebesgue de l'ombre est la même que la mesure de l'énergie du signal. Ce rapport illustre ce résultat en créant un nouveau type de granulométrie, qui est l'équivalent morphologique de l'analyse spectrale sur signaux complexes.

This page intentionally left blank.

Table of contents

Abstract	i
Résumé	ii
Executive summary	iii
Sommaire	v
Table of contents	vii
List of figures	ix
1 Introduction	1
2 Order relationship and Complementation	5
2.1 Properties of the order relationship	6
2.2 Order Relationship	8
2.3 Umbra	10
2.4 Maximum (\vee) and Minimum (\wedge)	10
3 Dilations and Erosions	12
4 Openings, Closings and Morphological Filters	13
5 Geodesy	18
5.1 Structuring element	23
5.2 Dilations and Erosions	23
5.3 Reconstructions	26
5.4 Openings and Closings by Reconstruction	29
5.5 Regional maxima and minima	30
5.6 Domes and Lakes	33
6 Top Hats	38
7 Morphological Gradients	38

8	Complex Watershed	42
9	Measurements	45
9.1	Basic Measurements and Minkowski Functionals	45
9.2	Granulometries and Pattern Spectra	47
9.3	Power Granulometry	49
9.3.1	Examples	50
10	Implementation Notes	57
11	Conclusion	58
	References	60

List of figures

Figure 1:	Extension of MM to complex signals by processing the real and imaginary parts separately. Top plot: amplitude. Bottom plot: phase in radians. Notice that new amplitudes and phases are created; amplitudes and phases that did not exist in the original signal. This violates the idea of maxima and minima of signals, which should not create new signal samples.	4
Figure 2:	The umbra of a single complex number, X , on the complex plane.	11
Figure 3:	Complex dilation on a test signal. Top: amplitude. Bottom: phase, in radians.	14
Figure 4:	Complex erosion on a test signal. Top: amplitude. Bottom: phase, in radians.	15
Figure 5:	Complex and classical dilation on a real chirped radar signal. First graph: Input. Second graph: classical dilation. Next graphs: structuring element diameters 8, 16, 32 samples.	16
Figure 6:	Complex and classical erosion on a real chirped radar signal. First graph: Input. Second graph: classical erosion. Next graphs: structuring element diameters 8, 16, 32 samples.	17
Figure 7:	Complex opening of a test signal. Top: amplitude. Bottom: phase, in radians.	19
Figure 8:	Complex and classical opening on a real chirped radar signal. First graph: Input. Second graph: classical opening, structuring element diameter is 9 samples. Next graphs: structuring element diameters 9, 17, 33 samples.	20
Figure 9:	Complex closing of a test signal. Top: amplitude. Bottom: phase, in radians.	21
Figure 10:	Complex and classical closing on a real chirped radar signal. First graph: Input. Second graph: classical closing, structuring element diameter is 9 samples. Next graphs: structuring element diameters 9, 17, 33 samples.	22
Figure 11:	Geodesic distance between X and Y . By convention, the distance between X and Z is infinite.	24

Figure 12: Complex geodesic dilation of $f(t)$ into $g(t)$, a geodesic mask. $f(t)$ is the function that features four impulses at samples 250, 500, 1000, 2250. The top graph is the amplitude and the bottom one is the phase.	27
Figure 13: Complex morphological reconstruction by dilation of mask $g(t)$ by marking function $f(t)$	28
Figure 14: Input spectrogram. The horizontal axis is the time and the vertical axis is the frequency. The units are arbitrary.	30
Figure 15: Complex horizontal opening with a horizontal (constant frequency) structuring element on a spectrogram. All structures that had a duration shorter than the duration of the structuring element were deleted.	31
Figure 16: Complex horizontal opening by reconstruction with the same structuring element as in Fig. 15. Notice that structures that were connected with the large constant frequency portion of the signal were preserved.	32
Figure 17: Regional maxima on a Fourier transform. The detection function is drawn with asterisks. Only the amplitude of the Fourier transform is shown.	34
Figure 18: The operation of a complex dome detector on a Fourier transform. Only the amplitude is shown.	36
Figure 19: Same as Fig. 18. λ is changed and the domes become larger. Only the amplitude is shown.	37
Figure 20: Complex white top hat on a Fourier transform. Top graph: Input and Output amplitudes. Middle graph: input phase in radians. Bottom graph: top hat phase.	39
Figure 21: Complex black top hat on a Fourier transform. Top graph: Input and Output amplitudes. Middle graph: input phase in radians. Bottom graph: top hat phase.	40
Figure 22: Illustration of morphological gradients on a 1-D profile.	42
Figure 23: Beucher gradient on a complex signal. First two graphs: amplitude and phase in radians of the test signals. Last two graphs: amplitude and phase in radians of the Beucher Gradient.	43

Figure 24: Complex Beucher gradient on a chirped (real) signal.	44
Figure 25: The complex watershed on a spectrogram. Left: the amplitude of the spectrogram, in gray scale. Right: the complex watershed of this spectrogram. The horizontal axis is the frequency while the vertical axis is the time. The units are arbitrary because it is a series of FFTs.	46
Figure 26: Simulated radar pulse. Period = 50 samples.	51
Figure 27: Power granulometry and power pattern spectrum of a simulated pulse. Period = 50 samples.	52
Figure 28: Power granulometry and power pattern spectrum of a simulated pulse. Period = 25 samples.	53
Figure 29: Pulse fragment, superposition of two tones (Period: 20 and 50 samples).	54
Figure 30: Power granulometry and power pattern spectrum of a simulated pulse. Superposition of two tones (Period: 20 and 50 samples). . .	55
Figure 31: Power granulometry and power pattern spectrum of a chirped radar pulse.	56

This page intentionally left blank.

1 Introduction

Mathematical Morphology is an image processing methodology which has been very successful in processing binary and gray-tone images. The goal of this report is to extend it to complex signals.

Complex signals are used in many fields. For instance, telecommunication signals use this type of representation routinely. Radio Frequency (RF) signals are mainly analyzed through their complex envelope and are understood in terms of their amplitude and phase – a complex quantity. Fourier transforms are intrinsically complex. Complex signals are multi-valued quantities. This feature is the main reason why it is difficult to properly extend mathematical morphology to such a class of signals.

The interpretation of these signals is radically different from the usual interpretation of gray-tone functions in black and white pictures. Complex signals are mainly characterized by their amplitude and then by their phase. Gray-tone signals are compared with each other with the usual order relationship that orders real numbers, that is, $x \leq y$. With this order relationship, negative values are smaller than zero; this is not the case for complex numbers. A negative value is interpreted as a phase shift of 180 degrees. In practice, gray-tone images rarely feature negative-valued pixels; complex signals do.

The information of gray-tone signals reside in the raw samples. Most of the time, complex signals represent the complex envelope of an RF signal. Complex signals are, in this case, the expression of the modulation of a carrier wave.

The average value of a signal, its DC value, is significant for pictures; it is related to the overall brightness of the image and it has a meaning for the human visual system. In contrast, the average value of complex signals is in general zero. The DC component of such a signal is considered parasitic and RF systems designers strive to eliminate it. The average value of a Fourier transform is also meaningless.

The most natural way to combine gray-tone signals is through set operations, such as the maximum, \vee , which is the equivalent of the set union \cup for binary images and through the minimum \wedge , equivalent to the intersection \cap for binary images. As Serra observed in [1], objects occlude each other in a scene and this type of combination is best described through set operations.

Complex signals are best combined using linear operators and are mostly understood through frequency-domain representations. So far, no alternate space representation exists for set operators. Set operators are therefore analyzed in the time domain or in the spatial domain.

There is usually a hierarchy of shapes in pictures. Objects include smaller objects;

objects are constructed from low level primitives. This was acknowledged very early in the field of computer vision, Marr's primal sketch [2] being one of the early examples of such combining. Edges were considered the basic primitives and those edges were combined to create more complex and semantically rich objects.

The idea of a hierarchy of shapes is rarely used in complex signals. In practice, the use of this idea is limited to the analysis of a signal with its harmonics, which constitute objects that are somehow lower in importance as compared to the fundamental frequency. The other use of the idea of hierarchy is to consider a signal with noise embedded in it. The hierarchy in both cases is based on relative signal intensities and relative bandwidths. It is hoped that the signal of interest has a narrower bandwidth or a higher intensity than the noise embedded in it; it is hoped that spurious signals have lower amplitudes than the fundamental frequency of the signal under consideration.

Although there is little use of the idea of hierarchy in complex signals, it is clear that there is a hierarchy that can be used to process such signals. For instance, communication signals are modulated at a fixed rate. Radar signals are modulated in amplitude, frequency and phase. Trying to understand the hierarchy in terms of Fourier analysis becomes rapidly futile because of the complexity of the resulting spectra.

Morphological techniques seem more appropriate for images than linear techniques. Linear techniques, on the other hand, seem better than morphological techniques for complex signals. One can then ask what can be gained by applying morphological or, for that matter, any non-linear technique to complex signals.

These tools open up more possibilities for signal processing, especially when the basic assumptions that are currently used start to break down. The main assumption is that signals are linearly combined. It is indeed the case for the propagation of signals in a medium. Yet, non-linearities exist at the transmission and at the reception of such signals. For instance, receivers are often saturated and transmitters over-driven. Moreover, most of the modulation techniques currently in use are non-linear because they use angle, or phase modulation.

More importantly, non-linearities are inevitable when one wishes to perform pattern recognition or decoding on such complex signals. A pattern recognition system destroys information. The amount of information processed as an input is usually six or seven orders of magnitude larger as compared to the amount of information that is produced at the output of such a system. It usually acquires megabytes of information and outputs a result that can be encoded by a few bits. Sometimes, the information is even reduced further to a single bit: pass/fail, present/not present. In general, linear systems do not destroy information; they change the way energy

and power are distributed in frequency. Therefore, pattern recognition is not possible without non-linearities.

The linear approach to information destruction is based either on quantization or on the idea that the noise floor is an immutable quantity. Using this approach, one suppresses frequency components by lowering their amplitudes either below a known quantization level or below the thermal noise floor. In either case the components disappear because they no longer influence the quantizer.

Morphological operators have more ways to control the destruction of information. They are controlled by size parameters, which has similarities with the frequency representation of signals. They are also controlled by shapes and they can perform template matching, not unlike matched filters. They are also controlled by topological properties of signals, which is a feature that has no equivalent in linear signal processing. Hierarchies can be built based on scale, intensity, inclusion and any combination of these properties.

It is therefore tempting to apply morphological operators on complex and RF signals. However, morphology needs to be adapted to the nature of such signals.

The simplest way to apply morphological operators to complex signals is to process the real and the imaginary components separately. Unfortunately, the results are disappointing. Considerable distortion of both phase and amplitude are introduced, as shown in Fig. 1. Phase and amplitudes that did not exist in the input signals are created and this is undesirable because the operators become unpredictable in terms of these important features.

Moreover, modifying operators in such a way solves only one part of the problem, that is, the implementation of morphological operators. There are other aspects that we need to consider: the complementation of signals, measurements and geodesy, which we will elaborate upon in this report.

The correct way of implementing morphology to complex signals is to create an order relationship between complex samples. Morphological operators are based on set operations: the Union $X \cup Y$, the Intersection, $X \cap Y$ and the set complement X^c . In the case of single-valued signals, the basic operators are the maximum $x(t) \vee y(t)$, the minimum $x(t) \wedge y(t)$ and the negation $-x(t)$. In both cases, the underlying concept is the order relationship. For sets, the relationship is the inclusion $X \subseteq Y$. For real numbers it is $a \leq b$. These two relationships create the union and the intersections for set operators and they create the maximum and the minimum for real numbers.

We therefore need to create an order relationship between complex numbers. This is, in theory, impossible because, as Barnett observed in [3], there is no natural way to order multi-valued quantities. Arbitrariness is unavoidable. However, it is still

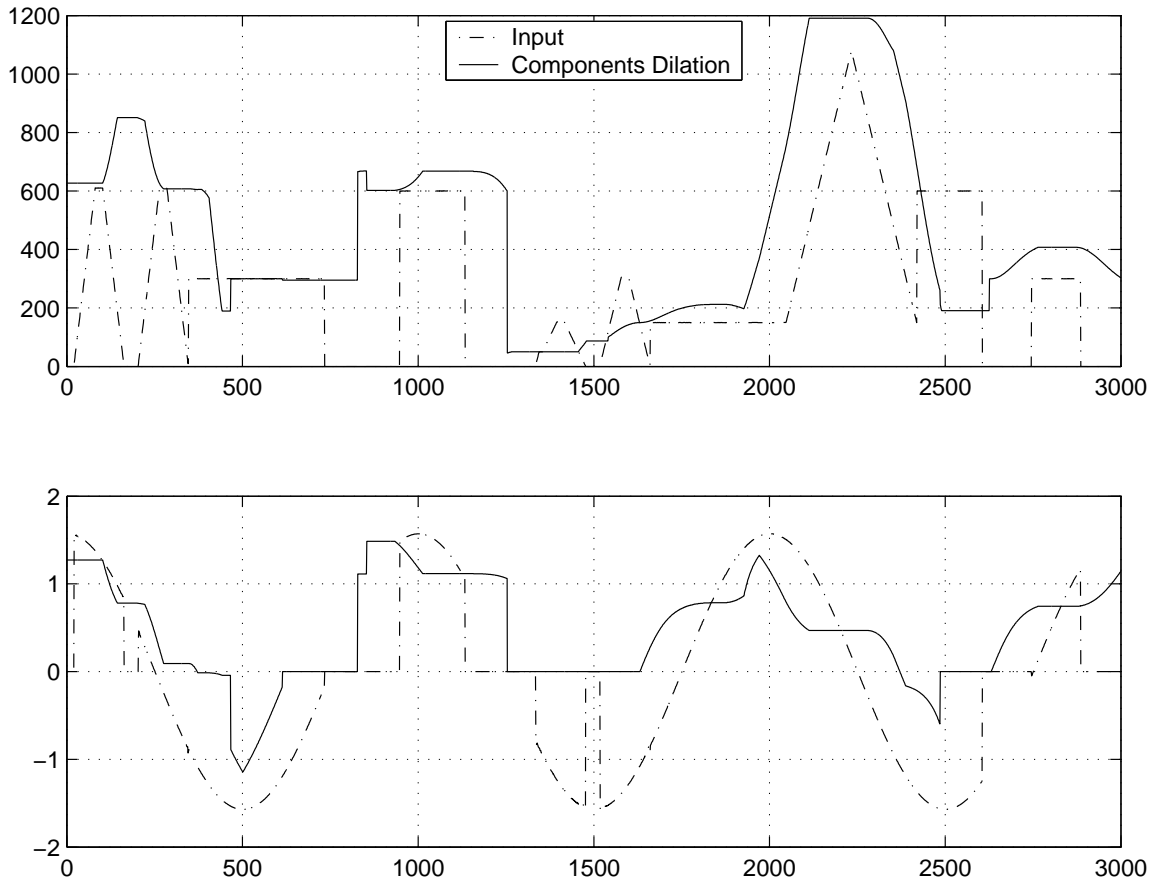


Figure 1: Extension of MM to complex signals by processing the real and imaginary parts separately. Top plot: amplitude. Bottom plot: phase in radians. Notice that new amplitudes and phases are created; amplitudes and phases that did not exist in the original signal. This violates the idea of maxima and minima of signals, which should not create new signal samples.

possible to realize such relationship by incorporating physical considerations in the process.

It is possible to create an order relationship that is specific to complex signals. There is no warranty that this relationship would ever be useful to other multi-valued quantities such as color images nor it is our goal to make a universal order relationship, if such relationship exists. The order relationship we propose is specific to signals that are best analyzed through their complex envelope.

In this report, we first create an order relationship and we verify that it is appropriate for the processing of complex signals. We then build upon this foundation by creating the basic morphological operators that make use of this order relationship. It turns out this order relationship can be applied to real signals, that is, signals with no imaginary component.

We then develop the concept of geodesy for complex signals, followed by the implementation of geodesic operators. This is followed by the complex watershed transformation, which might be used for segmenting Fourier transform images and time-frequency representations.

Morphological operators can be arithmetically combined and that creates top-hats and morphological gradients. RF and complex signals are quite different from gray-tone images. Not only the basic operators reflect these differences, but also the measurements that are performed on these signals are also different. These measurements are detailed in this report as well.

2 Order relationship and Complementation

Morphological operators are based on order relationships. However, there is no natural way of ordering complex numbers, as Barnett [3] observed, among others. Therefore, any order relationship among complex signals will be somewhat arbitrary. Yet, there are some guidelines we can use in order to design an order relationship which would be robust, physically relevant and reasonably implementable.

We first outline the criteria that make an order relationship appropriate to our specific context. We then propose a new order relationship that fulfills these criteria. We define the set complementation, based on this order relationship. As Serra did for gray-tone functions [4], we define the umbra on complex signals. Finally, we present the dilation and erosion operators, which constitute the basis onto which all the morphological operators are built upon.

There have been some extensions of morphology to color, or multi-valued images, Comer and Delp's work [5][6] being typical. They proposed two methods: the first

one was to perform standard morphological operations on each of the red (r), green (g) and blue (b) (RGB) components separately. The problem with this approach is that the transformations introduce values that do not exist in the input image. It is the same situation with complex signals. New phases and amplitudes would be created in an uncontrolled manner. Moreover, this method does not provide a strong enough formalism to assess and predict the behavior of such transformations. Their second approach partially corrected these problems. They transformed the vector-valued colors to a scalar, usually the Euclidean norm $d = \sqrt{r^2 + g^2 + b^2}$. They then used d to order pixels. They finally defined a maximum \vee and a minimum \wedge operator that used this order relationship. However, using a single scalar to order multivariate data has ambiguity problems. Two pixels with the same amplitude could very well not have the same color. Although Astola et al. [7] mentioned it was of little practical importance for color image processing, it is a different situation in communication signals, where we often strive to transmit and receive constant amplitude signals. Moreover, the relationship is not a total ordering because it violates the antisymmetry property: $a \leq b$ and $b \leq a$ implies $a = b$.

Talbot, Evans and Jones [8] suggested the use of a lexicographic order relationship for multi-valued morphology. They proposed simple and efficient algorithms that are appropriate for both quantized and continuous vectors. Chanussot and Lambert [9] proposed ordering relationships based on space filling curves. Both these approaches are vector-preserving, that is, they do not introduce values that do not exist in the input image. However, they are not directly applicable to complex signals.

2.1 Properties of the order relationship

This section enumerates the properties which should hold in order for our order relationship to be useful for the processing of complex signals. These properties take into account the specificities of complex signals.

$X \preceq Y$ is an order relationship between X and Y if the following properties hold:

Property 1

$$X \preceq X \text{ is true.} \tag{1}$$

Property 2

$$\text{If } X \preceq Y \text{ and } Y \preceq X \text{ then } X = Y. \tag{2}$$

Property 3

$$\text{If } X \preceq Y \text{ and } Y \preceq Z \text{ then } X \preceq Z. \tag{3}$$

Property 4 *Trichotomy law: one and only one of the following relationships holds, for all X and Y in \mathbb{C} .*

$$X \prec Y, X = Y, X \succ Y \quad (4)$$

When X , Y and Z are complex samples, we found that we should add the following properties, in order to improve the applicability of the order relationship.

Property 5 *The order relationship should be maintained under attenuation and gain variations λ .*

$$\text{If } X \preceq Y \text{ then } \lambda X \preceq \lambda Y, \lambda \in \mathbb{R}^+. \quad (5)$$

Property 6 *Scaling, translation and rotation invariance.*

The order relationship should only concern point-wise values. It should be invariant to scalings, that is, magnification factors and time scalings, as well as translations and rotations. Although scalings are similar in concepts to gain variations, they must be kept separate and also considered separately because their physical signification is radically different. A gain variation has no impact on the spatial aspects of a signal, for instance.

Property 7 *Comparing X to Y should yield the same result as comparing Y to X .*

This property eliminates implementations depending on the order into which the operands are applied.

$$X \preceq Y \text{ implies } Y \succeq X. \quad (6)$$

Property 8 *Signal statistics independence.*

The order relationship should be independent of the signal statistics. It should be a sample-to-sample, or point-wise relationship, regardless of the global characteristics of the signals under consideration. This property eliminates all the relationships that could rely on global measures such as averages. Not having this property could expose us to inconsistencies when processing signals with a DC bias. For instance, Barnett [3] suggested using a scalar function based on some distance measurement

between a sample and the average value of the dataset, which would be inapplicable to our context.

The first three properties make the total order relationship. Property 4 is not required to create an order relationship. However, we wish to make a relationship that features properties that are as close as possible to the properties of the usual order relationship between real numbers.

Property 5 is very important for signal processing, because gain variations are inevitable in the process of acquiring a signal. These gain variations have many causes and most of these causes conspire to make λ unknown. These include variations in amplifiers, propagation channel variations, variations in illumination sources and so on.

Property 6 seems fairly obvious. We wish to obtain a relationship that depends exclusively on the values of the samples. It is important to ensure independence between the order relationship and the spatial properties of the signals. The connection between the two is made by morphological operations through the use of structuring elements.

Property 7 eliminates order relationships that could be dependent on the order into which the operands are applied. It is indeed possible to devise such order relationship however these are not desirable in our context.

Statistical independence (Property 8) is important to us because it removes potential spatial dependencies. We do not wish to have an order relationship that varies from one set of signals to the next.

2.2 Order Relationship

In [10], we proposed an order relationship that satisfies these properties. $\Re(X)$ is the real part of complex number X . $\Im(X)$ is the imaginary part and $|X|$ is the amplitude of X .

$$X \preceq Y \text{ If: } \begin{cases} |X| < |Y| \\ \text{or} \\ |X| = |Y| \text{ and } \Re(X) < \Re(Y) \\ \text{or} \\ |X| = |Y| \text{ and } \Re(X) = \Re(Y) \text{ and } \Im(X) \leq \Im(Y). \end{cases} \quad (7)$$

We can also define a strict inequality based on this order relationship:

$$X \prec Y \text{ If: } \begin{cases} |X| < |Y| \\ \text{or} \\ |X| = |Y| \text{ and } \Re(X) < \Re(Y) \\ \text{or} \\ |X| = |Y| \text{ and } \Re(X) = \Re(Y) \text{ and } \Im(X) < \Im(Y). \end{cases} \quad (8)$$

Physically, signals which have more power than others should be considered larger. This is intuitively appealing in signal processing. Signals which have the same power level are considered larger than others if their real part is larger, in the usual sense. If signals are identical both for amplitude and for their real part, we then examine their imaginary part. The largest signal is then the one which has a positive imaginary component. This approach is somewhat arbitrary, especially when we put emphasis on the real component in the comparison. However, it is not possible to remove such arbitrariness.

For instance, we could have resolved the amplitude ambiguity by comparing phases instead of components. However, because phases vary between 0 and 2π , it is not possible to decide which phase is the largest without being arbitrary. Phase unrolling techniques could be devised, in order to free ourselves of the $0 - 2\pi$ circularity, but that would violate time translation and time scaling invariance, which would then make the order relationship impractical.

Speaking in terms of phase, for equal signal amplitudes, our order relationship arbitrarily decides that signals whose phases are closer to zero are larger. Signals that are symmetrically positioned with respect to the real axis are considered larger if their phases are between 0 and π .

When a signal is purely real, that is, when its imaginary component is zero, the order relationship degenerates into a simple comparison of the absolute values:

$$X \preceq Y \text{ If: } \begin{cases} |X| < |Y| \\ \text{or} \\ X \leq Y \end{cases} \quad X, Y \in \mathbb{R}. \quad (9)$$

Moreover, if a signal is real and positive, the order relationship degenerates into the same relationship used for gray-tone functions.

This order relationship is different from the usual relationship between real numbers. A negative X can be larger than a positive Y if $|X| > |Y|$, according to this relationship.

This new order relationship among real quantities is most useful in ordering AC signals. It turns out that this order relationship is useful for all the signals that are ordered in terms of their amplitudes instead of their real value. This class of signals usually consider the DC component an artifact. Audio signals, ultra sounds, RF and seismic signals are examples of such a class of signals.

2.3 Umbra

The umbra U of a real-valued function f is defined as the portion of space that is below the function, union with the function itself. For a single real-valued sample P , it is all the points of the real axis that are smaller than or equal to P . In the image processing practice, the signals are limited between $\pm M$, or between 0 and M , depending on the application.

The umbra of a complex sample X is similarly defined using our order relationship:

$$U = \{Y : Y \preceq X\} \quad (10)$$

Figure 2 illustrates graphically the umbra of a single sample on the complex plane. The umbra is the union of the following regions on the complex plane:

1. The interior of the circle centered on the origin and radius A .
2. The path on the the circle centered on the origin and radius A , starting from X , passing by $\theta = \pi$, and ending at X^* , X^* included if $\Im(X) > 0$.

2.4 Maximum (\vee) and Minimum (\wedge)

The max \vee and the min \wedge operators are defined:

$$X \vee Y = \begin{cases} X & \text{if } Y \preceq X \\ Y & \text{otherwise} \end{cases} \quad (11)$$

$$X \wedge Y = \begin{cases} Y & \text{if } Y \preceq X \\ X & \text{otherwise} \end{cases} \quad (12)$$

These operators are dimensionality-preserving [11], that is, they preserve the physical dimensions of the signals:

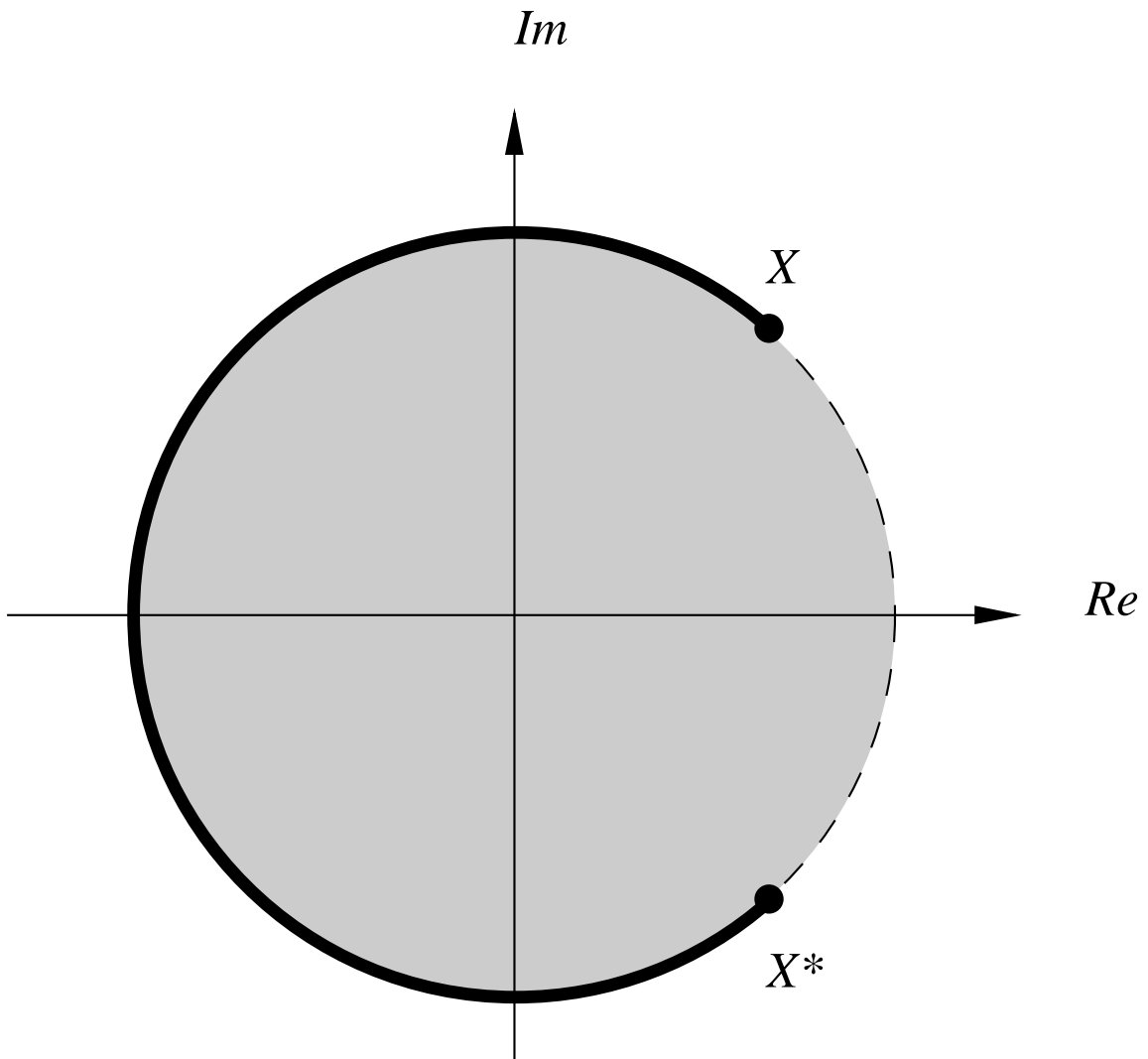


Figure 2: The umbra of a single complex number, X , on the complex plane.

$$\lambda X \wedge \lambda Y = \lambda(X \wedge Y), \lambda > 0 \quad (13)$$

$$\lambda X \vee \lambda Y = \lambda(X \vee Y), \lambda > 0. \quad (14)$$

This property is important because it ensures that the output of these operators have the same physical units as the units of the input signals. This property enables us to predict the properties of the output, when the signals are attenuated or amplified. The \vee and \wedge operators preserve the dimensionality of the input signal because they merely choose between two samples, based on their order relationship.

3 Dilations and Erosions

The dilation of a complex signal F by a flat structuring element B is denoted $\delta_B^C(F)$ and is defined as the maximum value of the translations of F by the vectors $-b$ of B , $\text{trans}_{-b}(F)$ [4]:

$$\delta_B^C(F) = \bigvee_{b \in B} \text{trans}_{-b}(F). \quad (15)$$

The erosion a complex signal F by the flat structuring element B uses the minimum instead of the maximum:

$$\epsilon_B^C(F) = \bigwedge_{b \in B} \text{trans}_{-b}(F). \quad (16)$$

It should be noted that the dilation and the erosion, using our order relationship, does not create new signal values. As it is the case with the scalar dilation and erosion, this transformation merely chooses among a certain number of samples the one that is the output.

These operators also preserve the dimensionality of the samples, exactly like they do for gray-tone images when we use flat structuring elements. This is because the operators \vee and \wedge preserve the dimensionality, as mentioned in Eqs. 13 and 14.

$$\lambda \delta_B^C(F) = \delta_B^C(\lambda F), \quad (17)$$

$$\lambda \epsilon_B^C(F) = \epsilon_B^C(\lambda F), \quad (18)$$

They also commute under spatial or time scaling, like their relatives in gray-tone and binary image processing. For signals, the time axis is t . For images, the image plane coordinates are (x, y) . In general, let \mathcal{K} be the coordinates, and $\lambda\mathcal{K}$ a uniform scaling λ over these coordinates. $F(\mathcal{K})$ is a function of coordinates \mathcal{K} , the dilation $\delta_B^C(F)(\mathcal{K})$ is also function of \mathcal{K} and so is $B(\mathcal{K})$:

$$\delta_B^C(F)(\lambda\mathcal{K}) = \delta_{B(\lambda\mathcal{K})}^C(F(\lambda\mathcal{K})), \quad (19)$$

$$\epsilon_B^C(F)(\lambda\mathcal{K}) = \epsilon_{B(\lambda\mathcal{K})}^C(F(\lambda\mathcal{K})), \quad (20)$$

where $F(\lambda)$ and $B(\lambda)$ denote spatial or time scaling on the image plane of signal F and structuring element B by the scaling factor λ . This is because such scaling is strictly a space/time operation.

Fig. 3 illustrates a dilation on a test signal, while Fig. 4 illustrates an erosion. Figs 5 and 6 illustrate the dilation and the erosion on a real radar signal used for ground mapping. The signal is chirped, that is, the frequency of the carrier wave at the beginning of the pulse is either higher or lower than the frequency at the end of the pulse. In this specific example, the size of the features in the signal tend to increase at the end of the radar pulse because the carrier frequency becomes lower at the end of the pulse.

4 Openings, Closings and Morphological Filters

Openings and closings are the basis of all morphological filters. Complex morphology is no exception. All the properties that are desirable for a filter are preserved in complex morphology.

A complex opening $\gamma_B^C(f)$ of complex signal f by the structuring element B is defined the same way as a classical morphological opening; it is an erosion followed by a dilation:

$$\gamma_B^C(f) = \delta_B^C(\epsilon_B^C(f)), \quad (21)$$

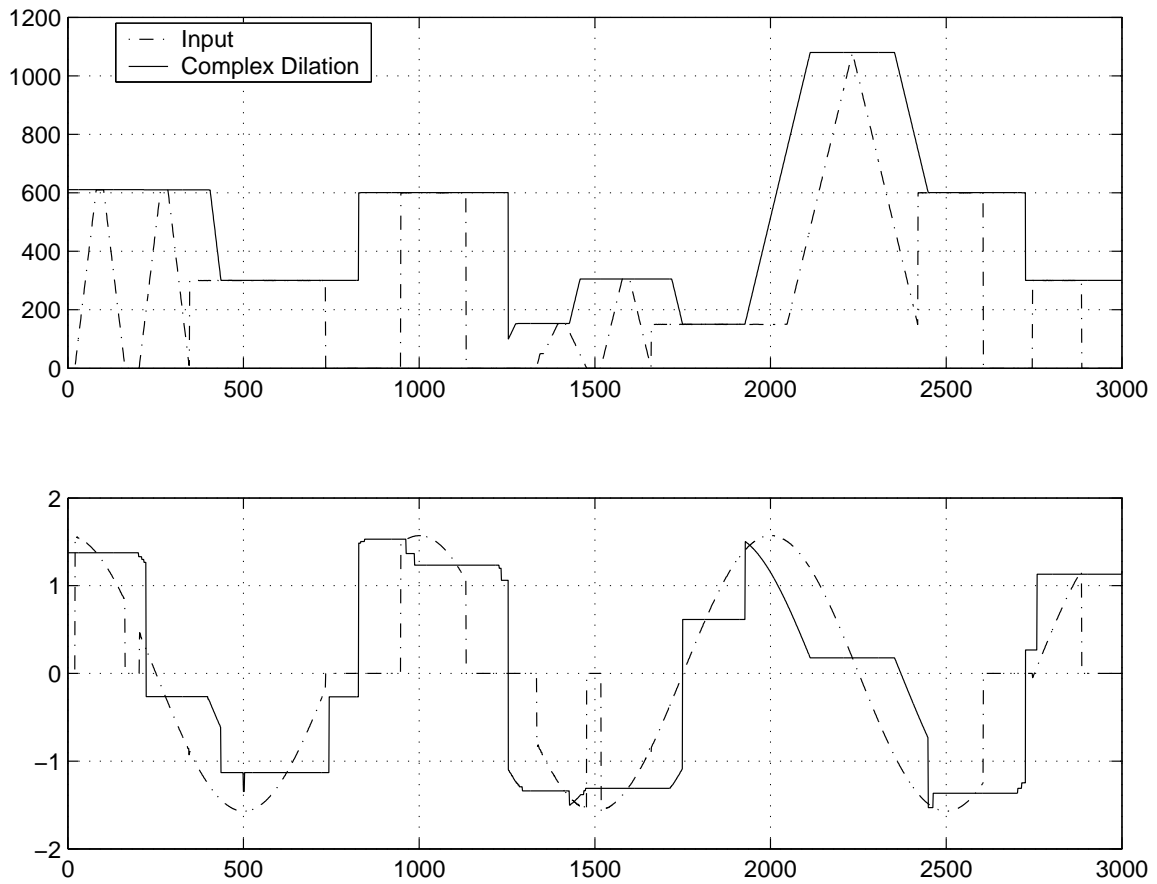


Figure 3: Complex dilation on a test signal. Top: amplitude. Bottom: phase, in radians.

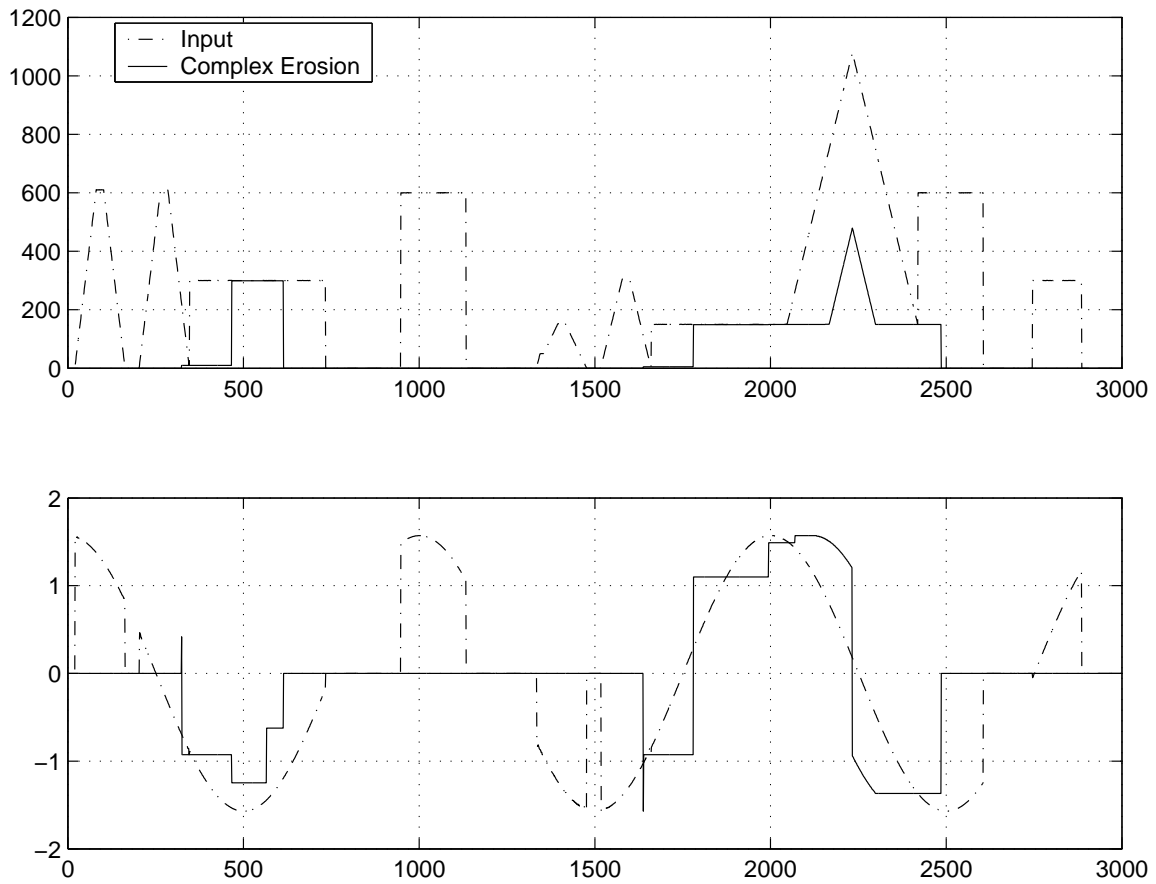


Figure 4: Complex erosion on a test signal. Top: amplitude. Bottom: phase, in radians.

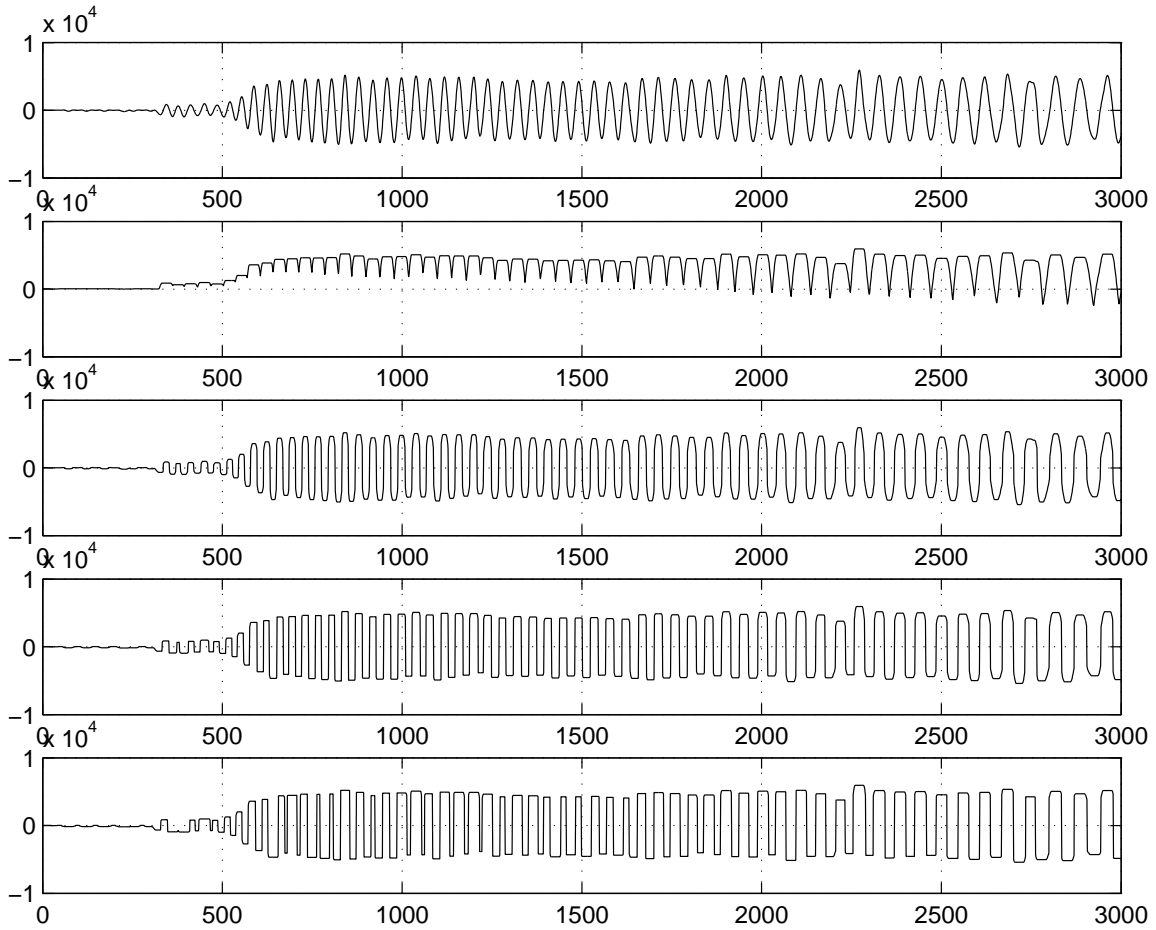


Figure 5: Complex and classical dilation on a real chirped radar signal. First graph: Input. Second graph: classical dilation. Next graphs: structuring element diameters 8, 16, 32 samples.

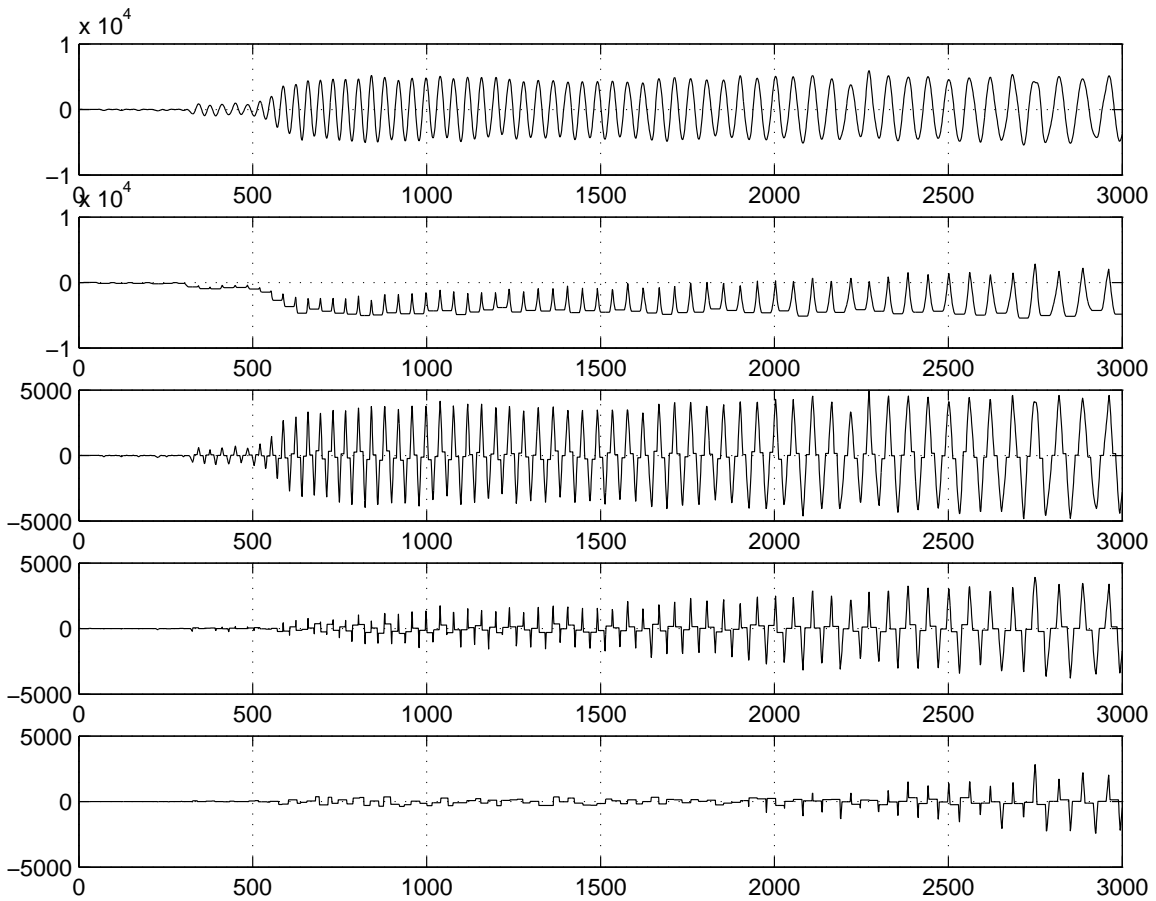


Figure 6: Complex and classical erosion on a real chirped radar signal. First graph: Input. Second graph: classical erosion. Next graphs: structuring element diameters 8, 16, 32 samples.

where B is the structuring element and \check{B} is the transposition of B . The transposition of B , \check{B} , is defined:

$$\check{B} = -b, b \in B, \quad (22)$$

where b are the vectors between the origin of structuring element B and every point of B .

Fig. 7 illustrates an example of such opening on a complex signal. Fig. 8 illustrates the result of a classical opening on a real signal, the chirped radar signal we used in Fig. 5 along with the complex opening. There are significant differences between the classical opening and the complex opening on the real signal. The classical opening is unsuitable to process such class of signals. It tends to increase the parasitic DC component in the signal, which is highly undesirable. This is caused by the fact that openings widen the valleys in signals. For RF signals the definition of a valley is based on the signal amplitude, or, in the case of real signals, on the signal's absolute value. The complex opening removes the whole waveform that is smaller than the structuring element, regardless of its polarity.

The complex closing is defined:

$$\phi_B^C(f) = \epsilon_{\check{B}}^C(\delta_B^C(f)). \quad (23)$$

It is the dual of the opening and it therefore works the same way as the opening on the complement of the signal.

Fig. 9 illustrates an example of a closing on a complex test signal while Fig. 10 on the chirped signal, along with its classical counterpart. The classical closing has the same problems as the classical opening, which is expected.

The complex opening and the complex closing feature the same properties as their classical counterparts; they are increasing and idempotent operators. The opening is anti-extensive while the closing is an extensive operator.

The opening and the closing are the two operators upon which morphological filters are built. Their complex counterparts can also be built using complex openings and complex closings in exactly the same way. Serra, in Ref [12] presents the most frequently used classical morphological filters. Their complex equivalent is relatively straightforward to develop. However, such extension is beyond the scope of this report.

5 Geodesy

Morphological operators are usually defined on \mathbb{R}^n , that is, in the Euclidean space such as the image plane. There is, however, a class of operators called “geodesic

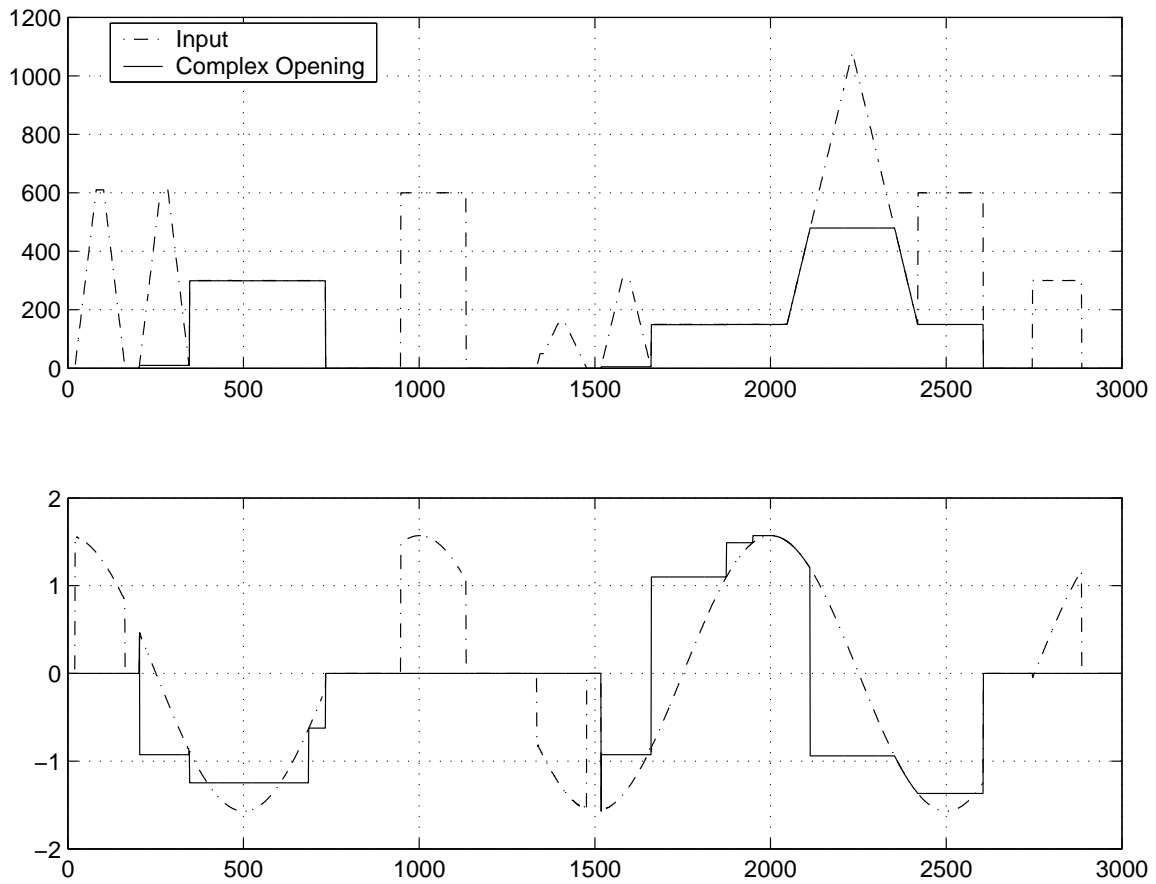


Figure 7: Complex opening of a test signal. Top: amplitude. Bottom: phase, in radians.

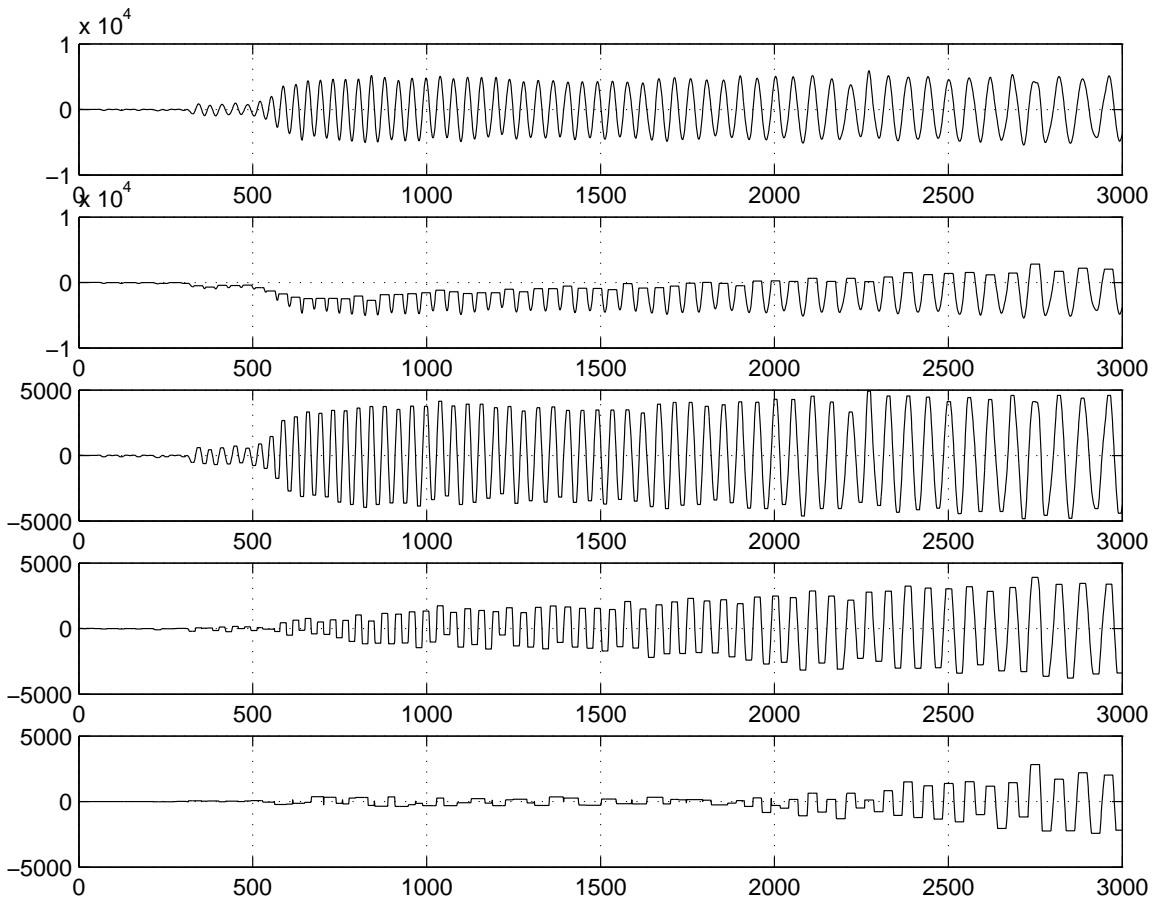


Figure 8: Complex and classical opening on a real chirped radar signal. First graph: Input. Second graph: classical opening, structuring element diameter is 9 samples. Next graphs: structuring element diameters 9, 17, 33 samples.

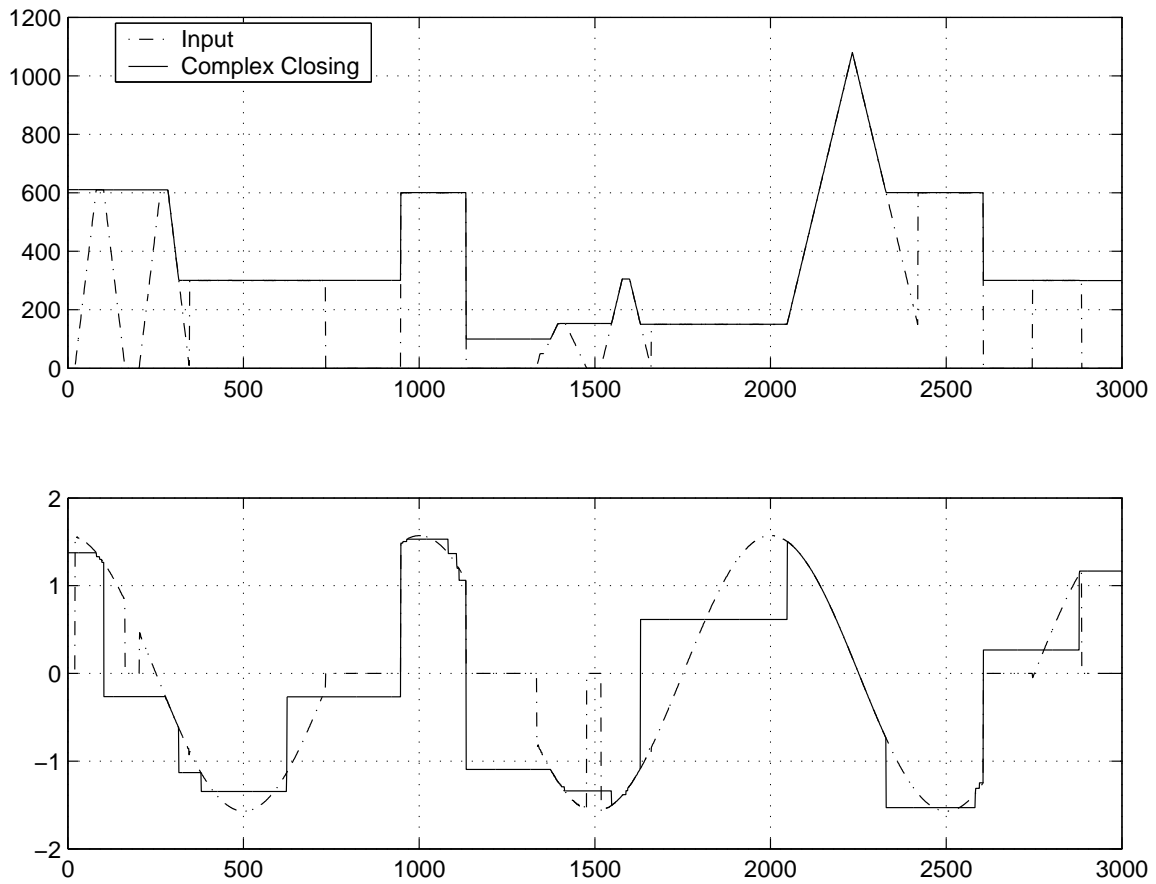


Figure 9: Complex closing of a test signal. Top: amplitude. Bottom: phase, in radians.

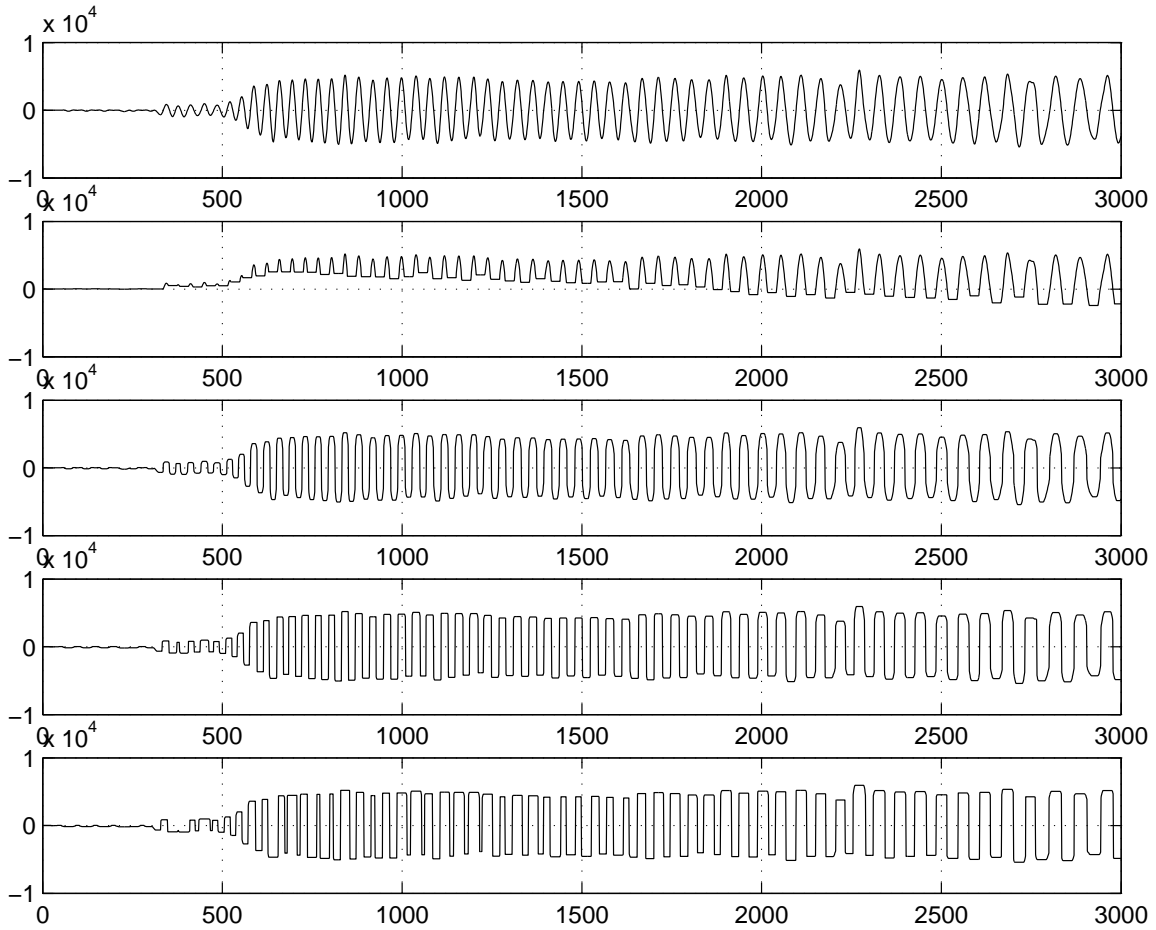


Figure 10: Complex and classical closing on a real chirped radar signal. First graph: Input. Second graph: classical closing, structuring element diameter is 9 samples. Next graphs: structuring element diameters 9, 17, 33 samples.

operators” which are defined in spaces where the Euclidean distance is replaced by a geodesic distance. These operators have been defined on both binary and gray-tone images. This section extends the concept of geodesy to complex signals.

Lantuéjoul and Beucher [13] first presented the concept of geodesy, applied to binary images. This concept has then been extended to gray-tone images with success, especially with the development of the morphological approach to segmentation, where it became its very basis. Beucher [14] and Meyer and Beucher [15] present an excellent overview on geodesy applied to functions and gray-tone image segmentation.

Euclidean morphology operates on the whole image plane, from $-\infty$ to ∞ . The Euclidean distance is the length of the shortest path between two points in this space. In geodesy, this space is partitioned by sets which are collectively referred to as a “geodesic mask”. These sets have arbitrary shapes. For instance, geodesic masks can have holes and disjoint particles. The geodesic distance in such a space is defined as the length of the shortest path between two points, the path being included in the geodesic mask. By convention, if the path is not included in the mask, the distance between the points is infinite. Fig. 11 illustrates the concept; $d(X, Y)$ is finite, while $d(X, Z)$ is infinite.

5.1 Structuring element

In Euclidean morphology, we frequently use a flat disk of radius ρ as a structuring element. In geodesy, ρ becomes a geodesic radius. Consequently, the shape of the structuring element changes, depending on the geodesic mask.

5.2 Dilations and Erosions

Geodesic dilations and erosions are defined in the same fashion as their Euclidean counterparts (Eqs. 15, 16). The difference resides in the translations, which become geodesic.

In Euclidean morphology, the iteration of a dilation or an erosion is equivalent to a single operator with a larger structuring element. It is also the case in geodesy. This property is important in Euclidean morphology because it allows the decomposition of large structuring elements into smaller parts. In geodesy, we use this property for the same reasons.

For instance, a Euclidean dilation with a disk of radius ρ can be implemented by iterating n times the dilation with a disk of radius e :

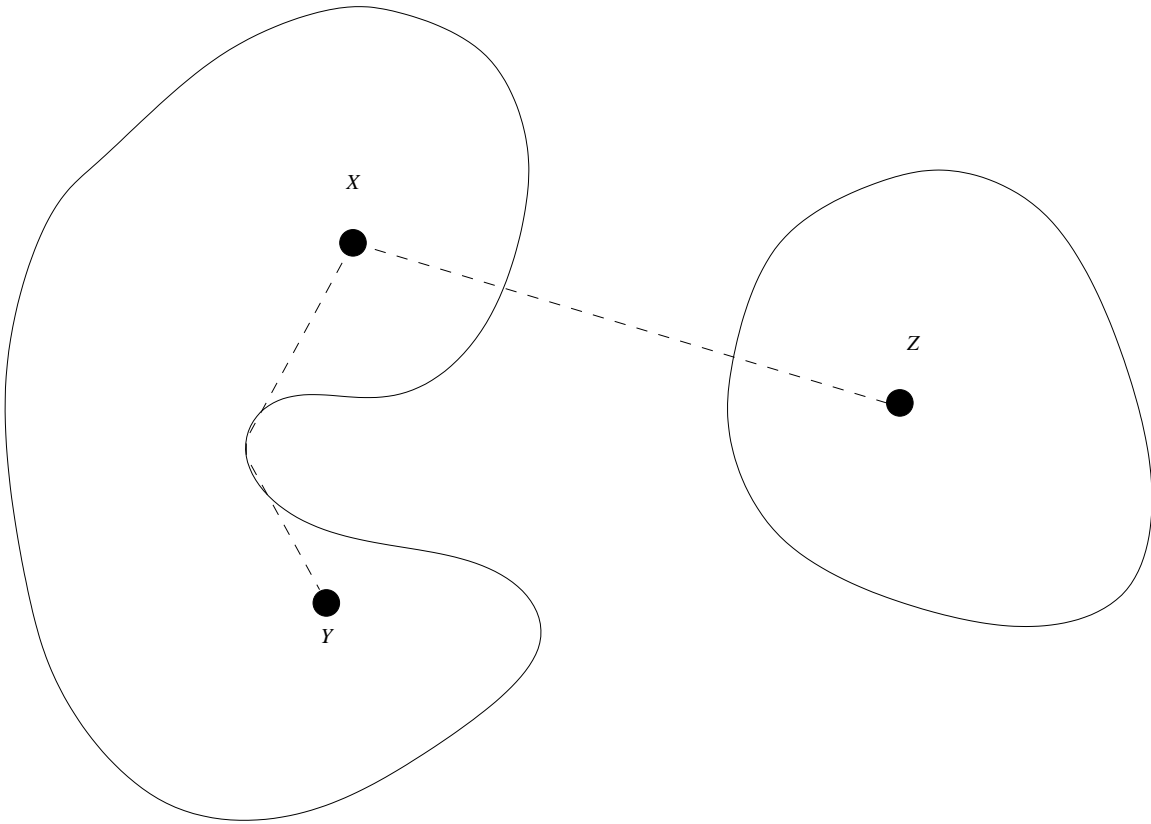


Figure 11: Geodesic distance between X and Y . By convention, the distance between X and Z is infinite.

$$\delta_\rho(X) = \underbrace{\delta_e(\dots \delta_e(\delta_e(X)) \dots)}_{\text{Iterated } n \text{ times}}, \quad (24)$$

with $n = \rho/e, \rho \geq e$.

This result is similar for erosions. It also suggests the following implementation, for a geodesic dilation, $\delta_\rho^G(X)$, of binary image X into a geodesic mask, G and a geodesic radius ρ :

$$\delta_\rho^G(X) = \lim_{e \rightarrow 0} \left[\underbrace{\delta_e(\dots \delta_e(\delta_e(X) \cap G) \cap G \dots)}_{n \text{ times}} \cap G \right]. \quad (25)$$

with $n = \rho/e, \rho \geq e$ and $X \subseteq G$.

The geodesic erosion is then:

$$\epsilon_\rho^G(X) = \lim_{e \rightarrow 0} \left[\underbrace{\epsilon_e(\dots \epsilon_e(\epsilon_e(X) \cup G) \cup G \dots)}_{n \text{ times}} \cup G \right]. \quad (26)$$

with $n = \rho/e, \rho \geq e$ and $X \supseteq G$.

The geodesic dilation with an infinitely small structuring element is identical to a Euclidean dilation followed by an intersection. By duality, the geodesic erosion with an infinitely small structuring element is identical to a Euclidean erosion followed by a union.

For functions and complex signals, the definitions are almost identical:

$$\delta_\rho^g(f) = \lim_{e \rightarrow 0} \left[\underbrace{\delta_e(\dots \delta_e(\delta_e(f) \wedge g) \wedge g \dots)}_{n \text{ times}} \wedge g \right]. \quad (27)$$

with $n = \rho/e$ and $f \preceq g$. The dilation is now complex and the intersection operator has been replaced by the complex minimum operator. $f \preceq g$ means that every point of complex function f is smaller (according to our order relationship) than its counterpart in function g .

The geodesic erosion is:

$$\epsilon_{\rho}^g(f) = \lim_{e \rightarrow 0} \left[\underbrace{\epsilon_e(\dots \epsilon_e(\epsilon_e(f) \vee g) \vee g \dots) \vee g}_{n \text{ times}} \right]. \quad (28)$$

with $n = \rho/e$ and $f \succeq g$. The erosion is complex and the union operator has been replaced by the complex minimum.

These two new geodesic operators have the same properties as their single-valued counterparts. This is because our relationship \preceq is an order relationship, and because the complement of a complex-valued function, as we defined it, reverses that order relationship. Figure 12 shows a geodesic dilation on a complex signal. The behavior of the amplitude is identical to gray-scale geodesic dilations. A dilation of f is carried out until it is constrained by the geodesic mask, as it is show in Fig. 12. The phase behavior, especially between samples 2000 and 2500, is caused by the unconstrained dilation of f in the center of the interval. Then, as $\delta_f()$ gets constrained by the geodesic mask, the output of the transformation is g instead of f .

5.3 Reconstructions

We define the morphological reconstruction by dilation of mask g by marker function f , $R_f^{\delta}(g)$, as the geodesic dilation of f inside g , using a geodesic disk whose radius ρ is infinite:

$$R_f^{\delta}(g) = \delta_{\infty}^g(f) \quad (29)$$

The dual operator of this type of reconstruction is the reconstruction by erosion, $R_f^{\epsilon}(g)$, defined as:

$$R_f^{\epsilon}(g) = \epsilon_{\infty}^g(f) \quad (30)$$

Eqs. 27 and 28 suggest we iterate geodesic dilations and erosions until idempotence, that is, until no change occur from one iteration to the next. It is however preferable to use either recursive algorithms, or Vincent's [16] [17] fast sequential algorithms, which were designed for generic computer architectures. The extension of these algorithms to complex signals is trivial. Fig. 13 shows an example of complex reconstruction by dilation.

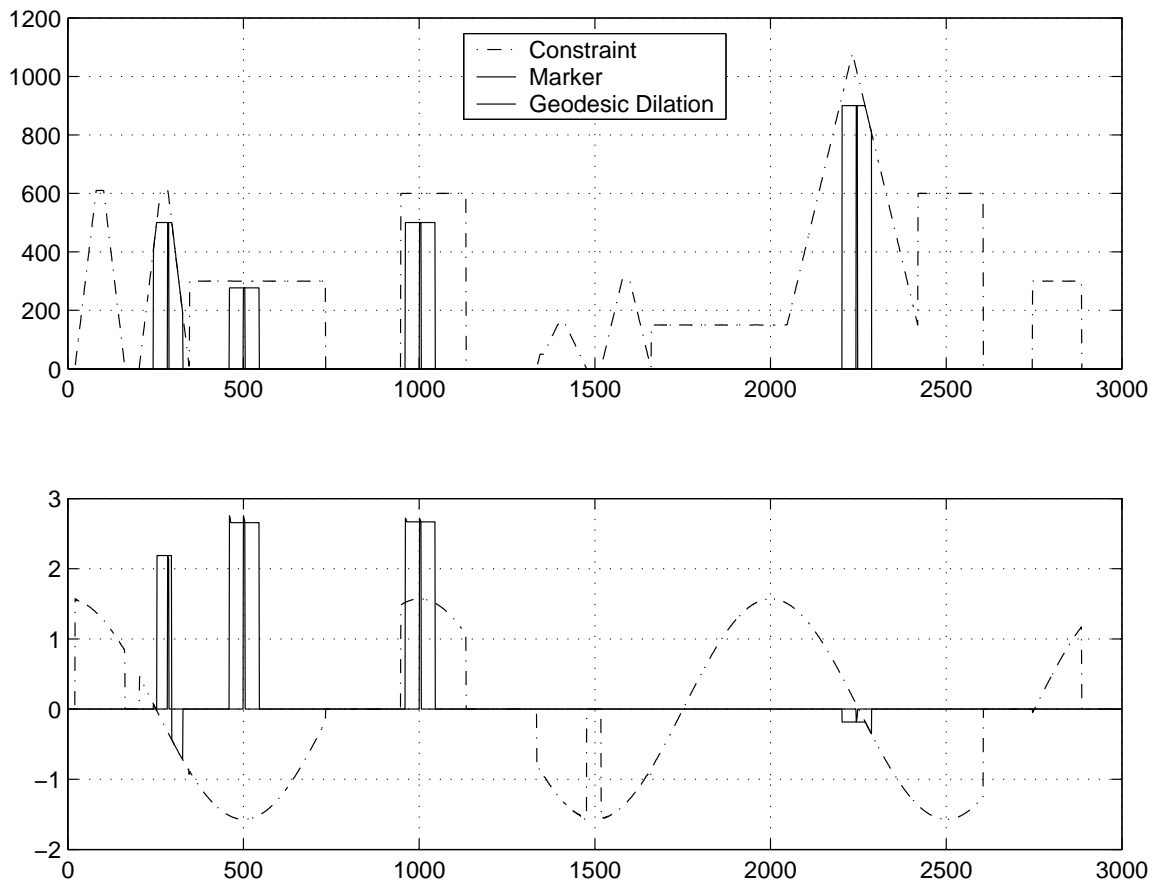


Figure 12: Complex geodesic dilation of $f(t)$ into $g(t)$, a geodesic mask. $f(t)$ is the function that features four impulses at samples 250, 500, 1000, 2250. The top graph is the amplitude and the bottom one is the phase.

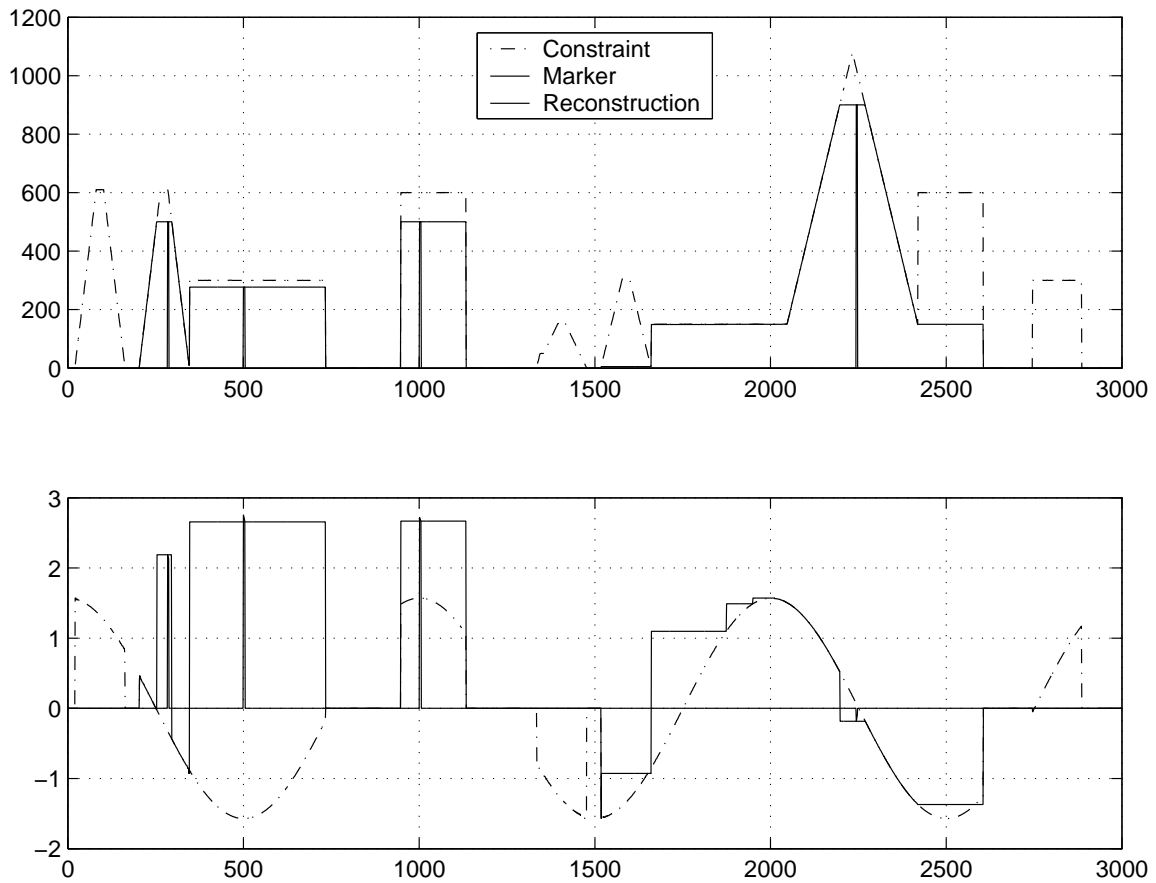


Figure 13: Complex morphological reconstruction by dilation of mask $g(t)$ by marking function $f(t)$.

A reconstruction by dilation preserves the geodesic mask maxima that have been marked by the function to be dilated. Reconstructions by erosion preserve minima in the same way. Reconstructions are invariant to scaling, amplitude and shapes. These operators depend on the topological properties of objects.

5.4 Openings and Closings by Reconstruction

The morphological opening is an erosion, followed by a dilation:

$$\gamma_B(f) = \delta_{\check{B}}(\epsilon_B(f)), \quad (31)$$

where B is the structuring element and \check{B} is the transposition of B .

The opening by reconstruction replaces the dilation with a reconstruction by dilation:

$$\gamma_B^R(f) = R_{\epsilon_B(f)}^\delta(f). \quad (32)$$

The morphological closing is defined:

$$\phi_B(f) = \epsilon_{\check{B}}(\delta_B(f)). \quad (33)$$

The closing by reconstruction is:

$$\phi_B^R(f) = R_{\delta_B(f)}^\epsilon(f). \quad (34)$$

These operators have been defined on binary and gray-tone images. Their definition on complex signals is the same. Dilations, erosions and reconstructions become complex operations. Figs 14–16 shows an example of such an opening on a spectrogram, which is a sequence of overlapped Fast Fourier Transforms (FFT). On that example, we used a horizontal structuring element. The complex morphological opening preserved the horizontal components, that is, the spectrogram sections where the signal had a constant frequency. The opening by reconstruction also preserved all the components that were connected to these constant frequency sections. The structuring element length was 201 time samples. It should be noted that the higher frequency component at the bottom of the spectrogram has not been fully removed by the opening by reconstruction. This is because there is low amplitude connected path between the horizontal segment approximatively starting at sample 1500 and the high frequency component of the signal. This path is caused by the brutal frequency transition of the low frequency component of the signal at that time; such a

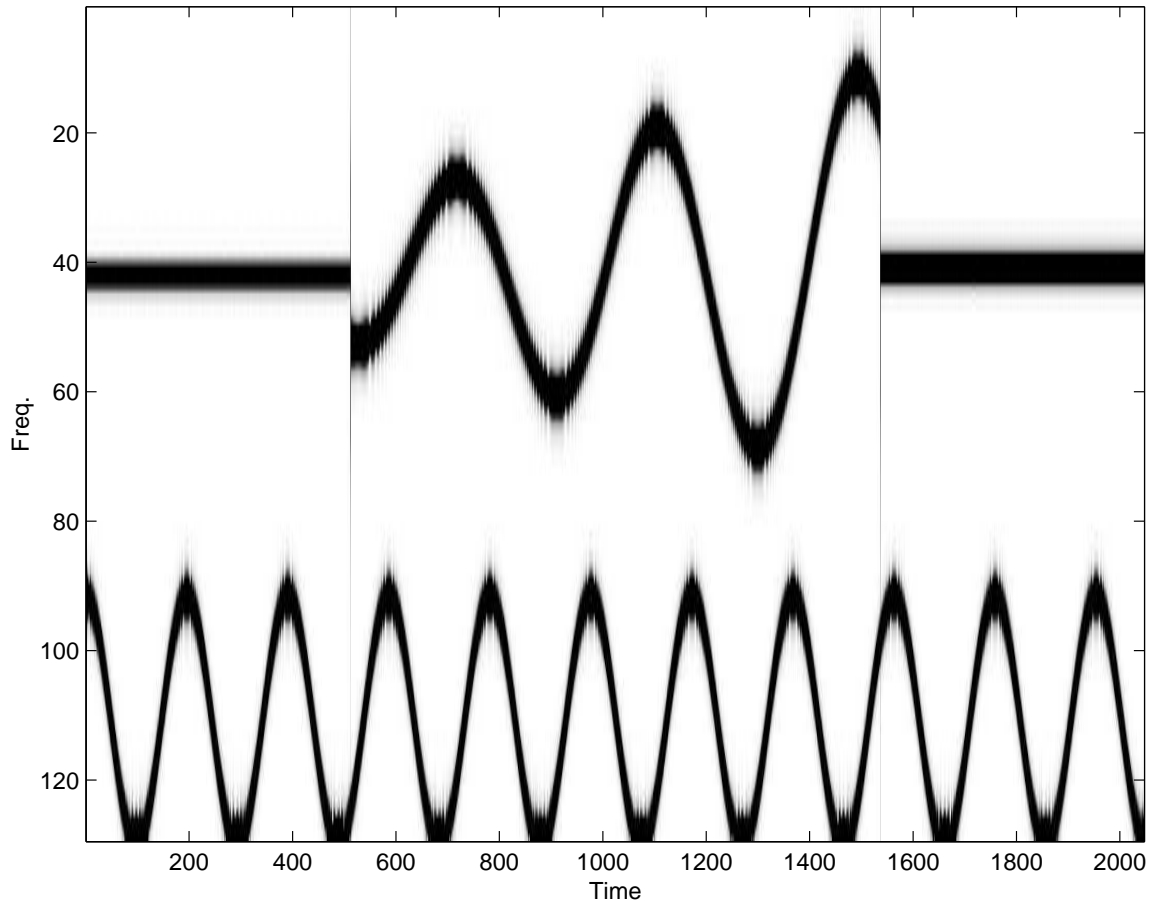


Figure 14: *Input spectrogram. The horizontal axis is the time and the vertical axis is the frequency. The units are arbitrary.*

transition widened the spectrum and spread the spectral power over the whole FFT. This clearly shows that the reconstruction is scale-independent. That transition is over a single FFT; an event two orders of magnitude smaller than the scale of the structuring element.

The complex opening by reconstruction has the same properties as its gray-tone counterpart: idempotence, anti-extensivity, increasing and duality with complex closing by reconstruction. Openings and closings by reconstruction better preserve the shapes than their morphological counterparts.

5.5 Regional maxima and minima

Beucher [14], defined the regional maximum as a plateau, that is, a region of constant value, which can only be accessed through ascending paths. A regional minimum is

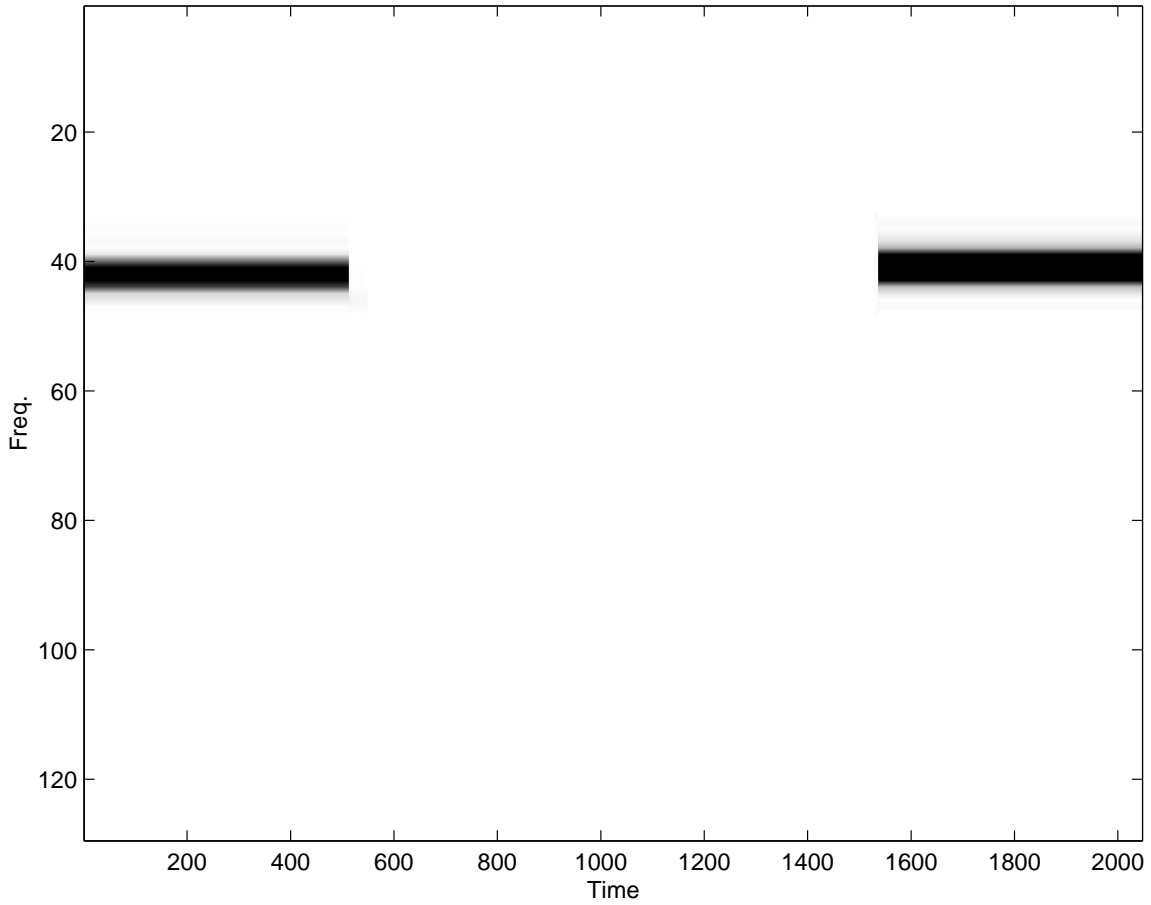


Figure 15: Complex horizontal opening with a horizontal (constant frequency) structuring element on a spectrogram. All structures that had a duration shorter than the duration of the structuring element were deleted.

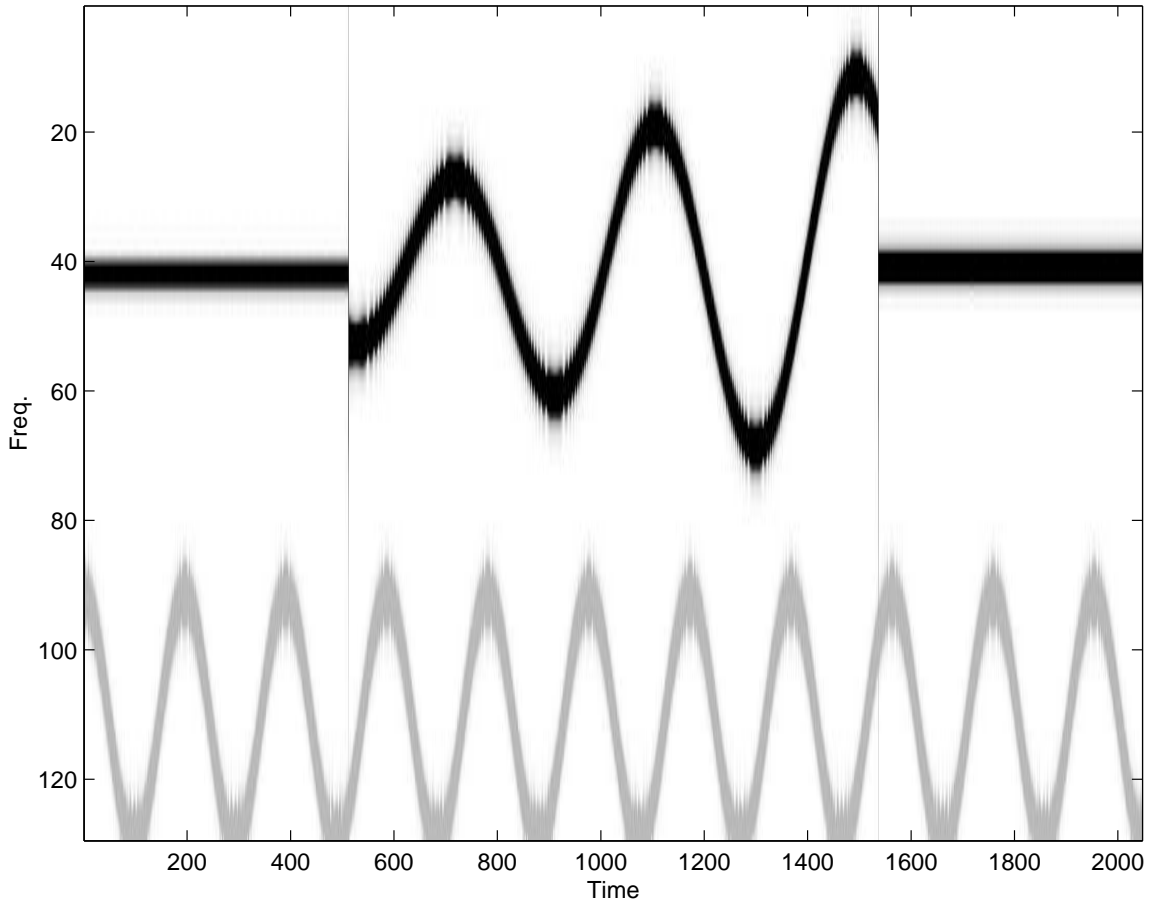


Figure 16: Complex horizontal opening by reconstruction with the same structuring element as in Fig. 15. Notice that structures that were connected with the large constant frequency portion of the signal were preserved.

a plateau accessible through descending paths only.

The idea of ascending or descending paths is of course dependent on the order relationship used. Regional maxima and minima can be extended to complex signals by using the complex order relationship. Classically, these objects are detected using reconstructions.

For gray-tone pictures, the regional maxima of f , $\mathbf{Rmax}(f)$, is composed of all the points x such that:

$$\mathbf{Rmax}(f) = \{x : f(x) \neq R_{f-\epsilon}^\delta(f)\}, \quad (35)$$

where ϵ is a small value, tending towards 0.

Similarly, regional minima are detected:

$$\mathbf{Rmin}(f) = \{x : f(x) \neq R_{f+\epsilon}^\epsilon(f)\}. \quad (36)$$

These definitions have to be modified for complex morphology, because our order relationship is not the same as it is in gray-scale morphology. For gray-scale signals, $f - \epsilon < f, \epsilon > 0$. This is generally not true for complex signals.

We therefore propose the following definitions for the complex regional minima and maxima:

$$\mathbf{Rmax}(f) = \{x : f(x) \neq R_{\lambda f}^\delta(f)\}, \quad (37)$$

where $\lambda \in \mathbb{R}^+, f(x) \in \mathbb{C}^n$ and $\lambda \rightarrow 0$.

$$\mathbf{Rmin}(f) = \{x : f(x) \neq R_{(1+\lambda)f}^\epsilon(f)\}. \quad (38)$$

Fig. 17 shows an example of regional maxima detection on a Fourier transform. For the purpose of clarity, only the amplitude of the Fourier transform is shown.

5.6 Domes and Lakes

The algorithms used to find regional maxima and minima are extended by using arbitrary ϵ . In gray-scale morphology, these extensions are called “domes” and “lakes”:

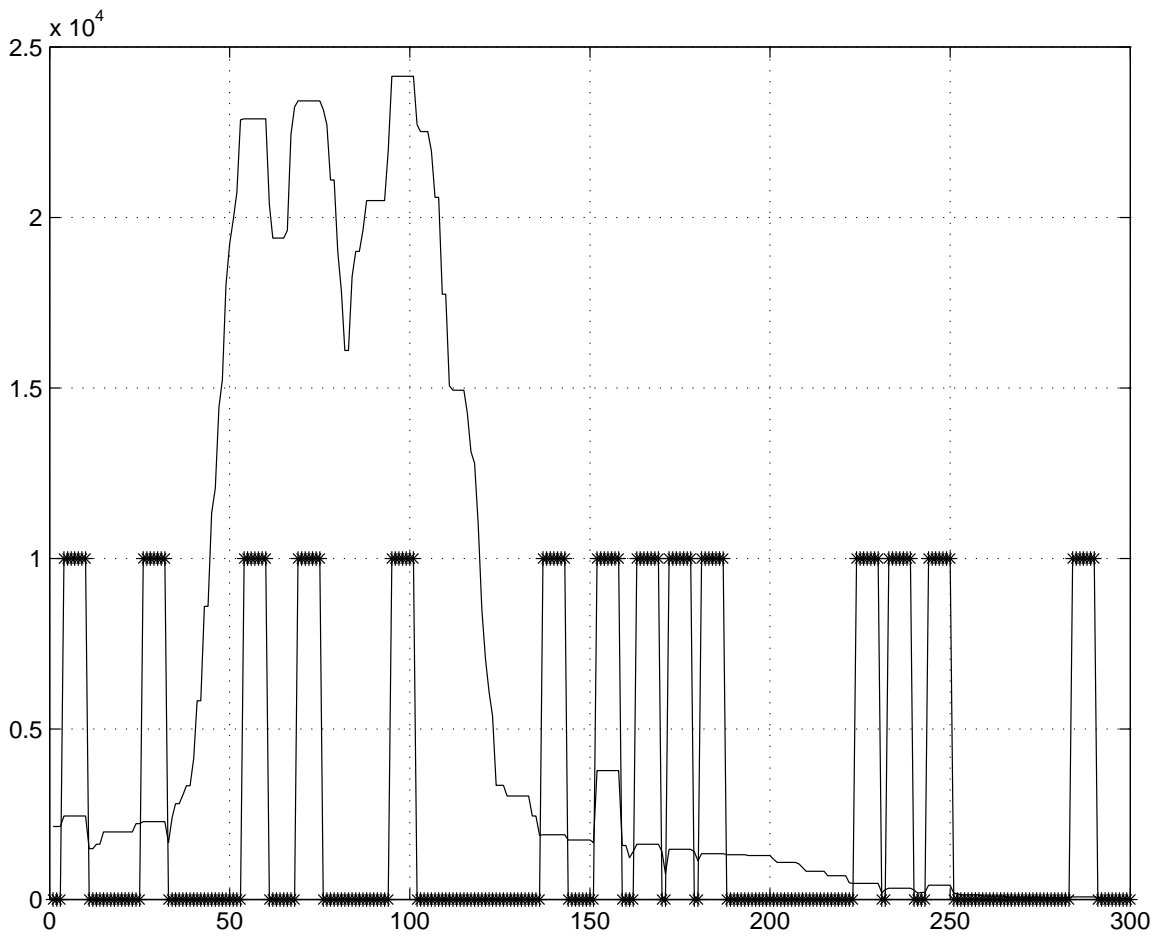


Figure 17: Regional maxima on a Fourier transform. The detection function is drawn with asterisks. Only the amplitude of the Fourier transform is shown.

$$\mathbf{Dome}_h(f) = \{x : f(x) \neq R_{f-h}^\delta(f)\}, \quad (39)$$

where $h \in \mathbb{R}^+$, $f(x) \in \mathbb{R}^n$.

$$\mathbf{Lake}_h(f) = \{x : f(x) \neq R_{f+h}^\epsilon(f)\}. \quad (40)$$

Regional maxima and minima are sensitive to noise. Noise introduces small extraneous maxima and minima in signals. If the noise level is known, dome detectors can alleviate this problem by merging together maxima that are separated by altitude variations smaller than h . Lake detectors also perform in the same fashion on signal minima.

Complex domes and lakes are an extension of complex regional maxima and minima:

$$\mathbf{Dome}_\lambda(f) = \{x : f(x) \neq R_{\lambda f}^\delta(f)\}, \quad (41)$$

where $\lambda \in]0, 1]$, $f(x) \in \mathbb{C}^n$.

$$\mathbf{Lake}_\lambda(f) = \{x : f(x) \neq R_{(1+\lambda)f}^\epsilon(f)\}. \quad (42)$$

Fig. 18 shows an example of a complex dome detector on the same Fourier transform used in Fig. 17. Fig. 19 shows the effect of changing λ .

Geodesic operators are controlled by topological parameters. The marker function that controls the reconstruction of objects is such a parameter. This example illustrates how the idea of connectedness is used to manipulate signals. In this report, the idea of connected paths has been extended from gray-tone functions to complex signals by modifying the usual order relationship.

Minima, maxima, domes and lakes detectors are another type of operator that merges the idea of signal intensity and topology. Openings and closings by reconstruction are a class of operators that combine both the idea of topology with the idea of scale or shape through the use of a structuring element.

Topological operators are very robust because they are scale and intensity invariant.

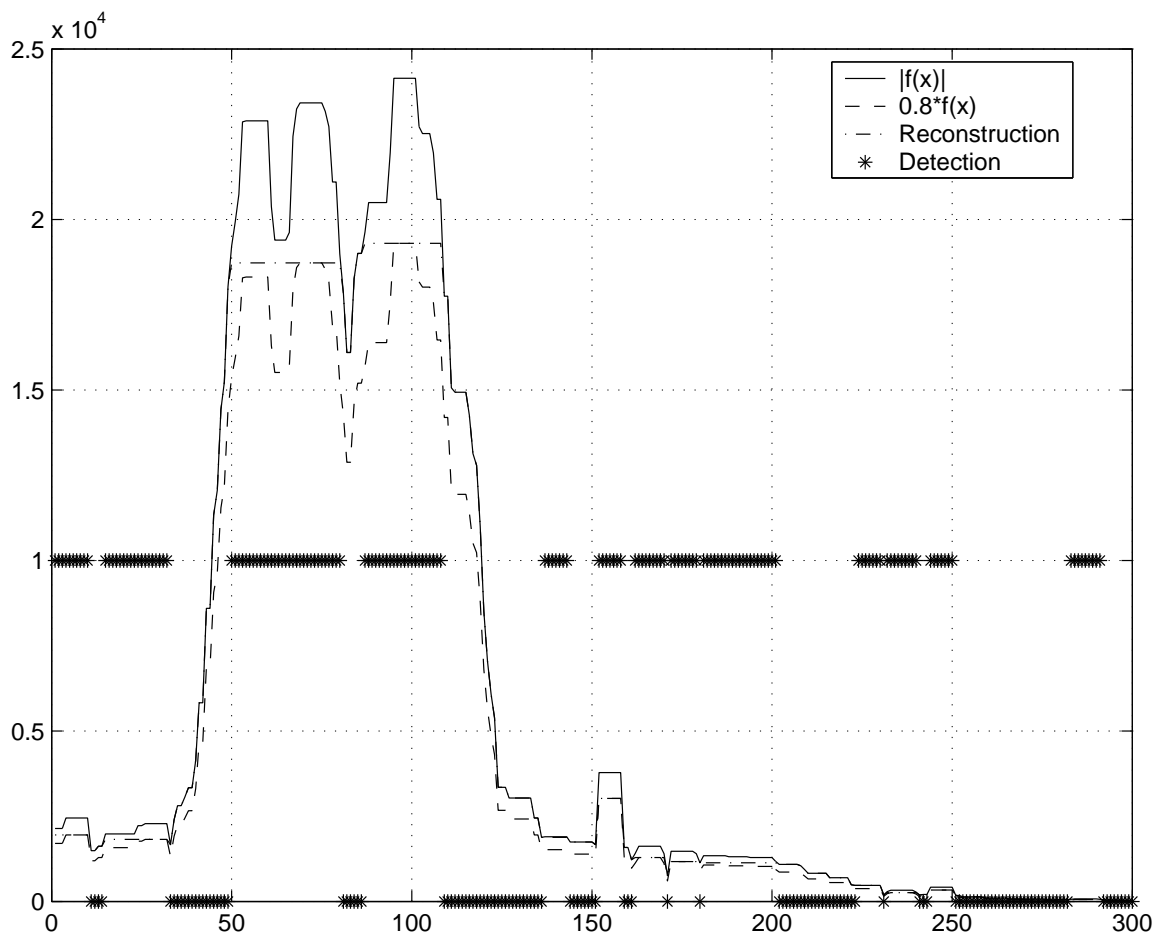


Figure 18: The operation of a complex dome detector on a Fourier transform. Only the amplitude is shown.

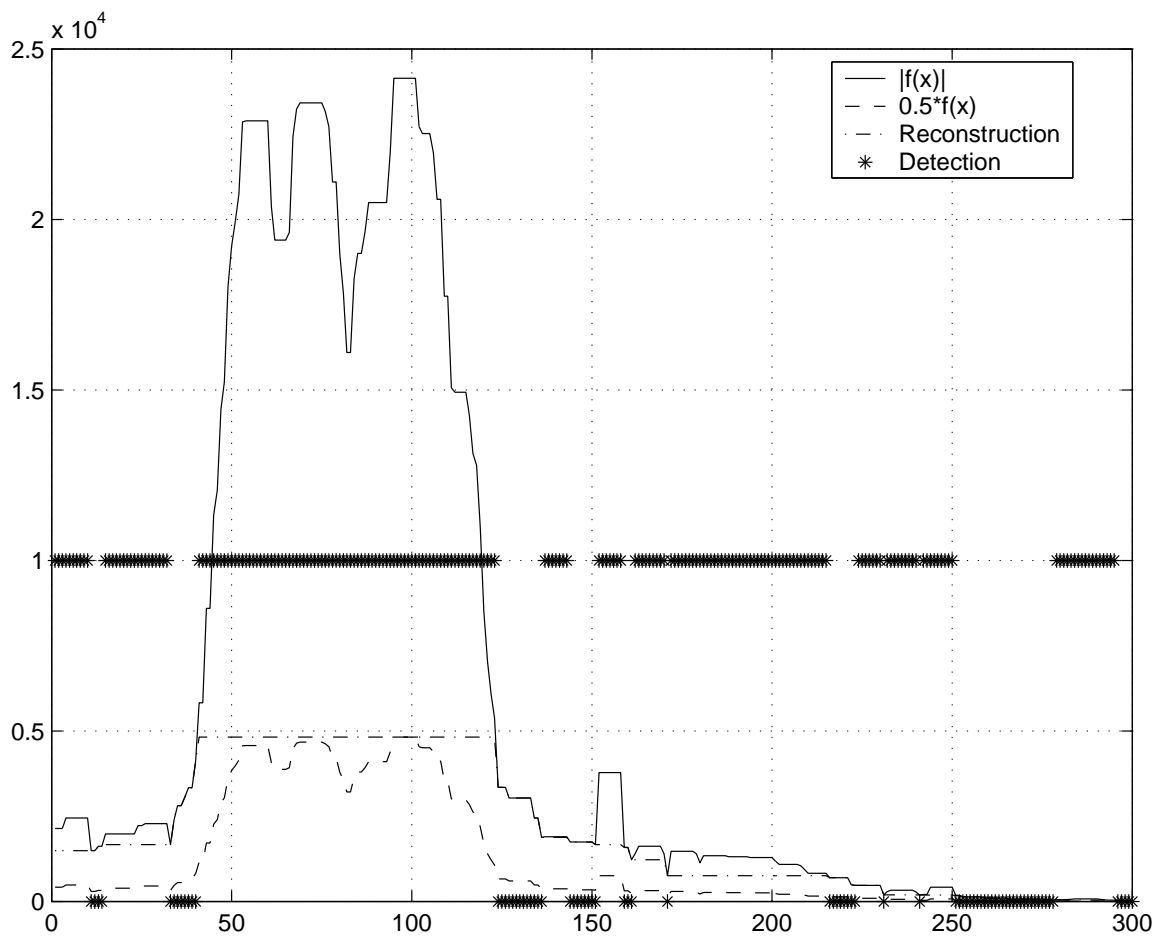


Figure 19: Same as Fig. 18. λ is changed and the domes become larger. Only the amplitude is shown.

6 Top Hats

Openings and closings suppress objects that are smaller than the structuring element. These have an effect that is similar to low-pass filters. Top hats, invented by Meyer in [18] and also described in Serra [4] are the equivalent of high-pass filters.

There are two types of top hat transformations: the white and the black top hat. The white top hat with structuring element B is defined:

$$\mathbf{wTop}_f(B) = f - \gamma_f(B). \quad (43)$$

The opening removes small bright peaks in f ; the difference between f and the opening then enhances the very peaks that were removed by the opening.

The black top hat is defined:

$$\mathbf{bTop}_f(B) = \phi_f(B) - f. \quad (44)$$

This top hat enhances minima that are smaller than the structuring element B . It should be noted that these minima appear as maxima because of the order in which the subtraction is done.

These definitions do not fundamentally change for complex signals. It is simply a matter of using complex openings and closings instead of the classical operators.

These two transformations, coupled with thresholding, are often used as peak detectors. Fig. 20 shows an example of a white top hat applied on the Fourier transform of a chirped radar signal. Fig. 21 shows an example of a black top hat on the same signal. It should be noted that this operator creates new amplitudes and phases because of the arithmetic operation. As we can see in Figs 20 and 21, the operation is neither extensive nor anti-extensive. The size of the structuring element in both examples is 11 samples in length. In Fig. 20, all the amplitude peaks smaller than 11 samples were enhanced. In Fig. 21, all the amplitude valleys were inverted and enhanced by the black top-hat. Openings and closings by reconstruction are also used to create top hats. These are called reconstruction top hats.

7 Morphological Gradients

Gradients are operators frequently used in segmentation because they enhance variations in signals. In images, these variations are assumed to be edges. Beucher invented

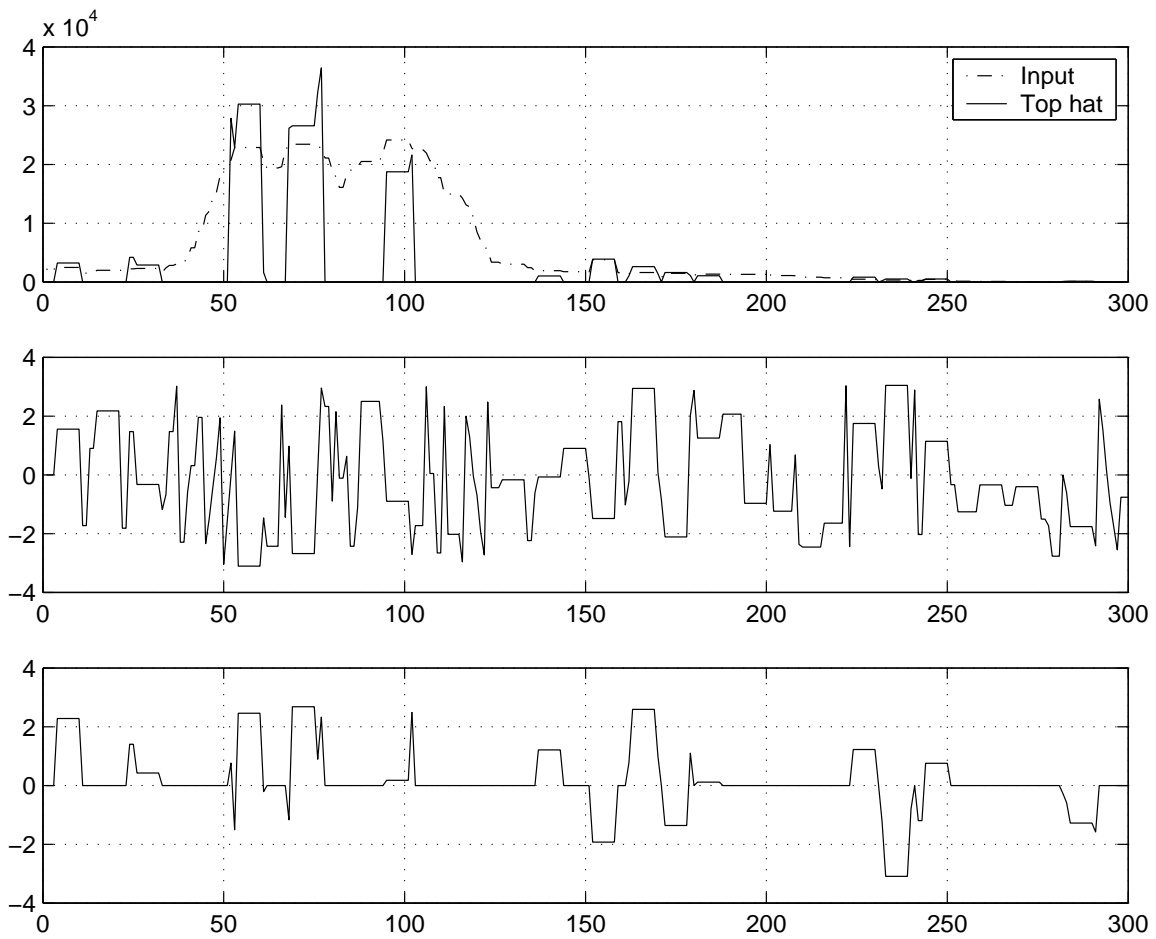


Figure 20: Complex white top hat on a Fourier transform. Top graph: Input and Output amplitudes. Middle graph: input phase in radians. Bottom graph: top hat phase.

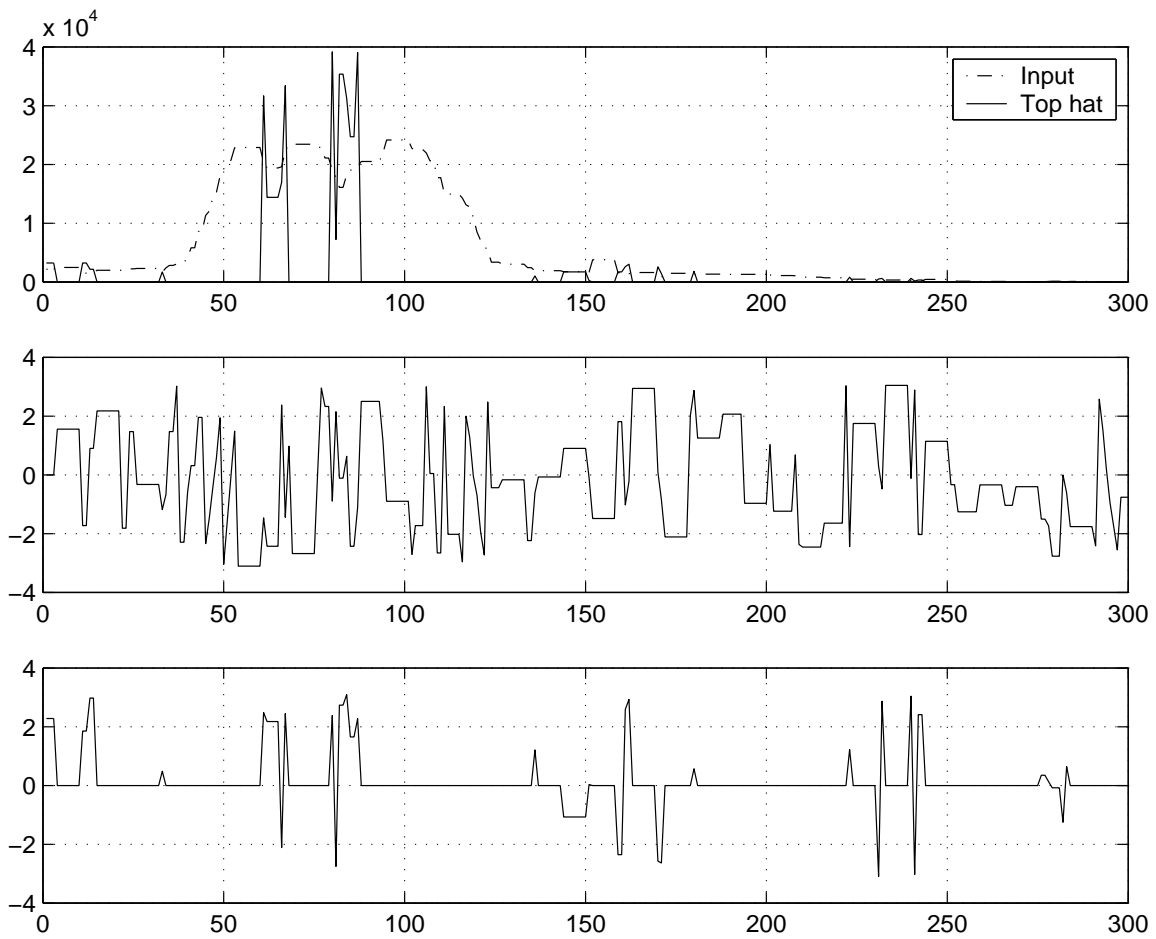


Figure 21: Complex black top hat on a Fourier transform. Top graph: Input and Output amplitudes. Middle graph: input phase in radians. Bottom graph: top hat phase.

the morphological gradient and described its various aspects in [14]. A survey of the various morphological gradients is available in [19].

Morphological gradients are based on three different combinations of operators:

- Arithmetic difference between a dilation and an erosion with the same structuring element B :

$$\mathbf{Mg}_B(f) = \delta_B(f) - \epsilon_B(f). \quad (45)$$

This is the morphological gradient, also called the Beucher gradient.

- Difference between a dilation and the input function f :

$$\mathbf{Eg}_B(f) = \delta_B(f) - f. \quad (46)$$

This is called the external gradient.

- Difference between the input function f and an erosion dilation:

$$\mathbf{Ig}_B(f) = f - \epsilon_B(f). \quad (47)$$

This is called the internal gradient.

In digital images, the edges have to be located on the pixels. The edges are either on the external contours of the shapes or on the internal contours or on both. This gradient generates the external edges. Usually, the size of the structuring element is as small as possible. In the continuous case, when B is infinitesimally small, the distinction between the three basic types of gradients vanishes and Beucher demonstrated in [14] that it was the same as the gradient modulus $|\nabla f(x)|$, where

$$\nabla f(x) = \left(\frac{\partial f}{\partial x_1}, \frac{\partial f}{\partial x_2} \right)$$

in the image plane.

Fig. 22 illustrates the morphological gradient on a 1-D profile. Complex morphological gradients use the same definitions. Fig. 23 shows the application of a complex Beucher gradient on a signal, while Fig. 24 shows a Beucher gradient on a chirped radar signal.

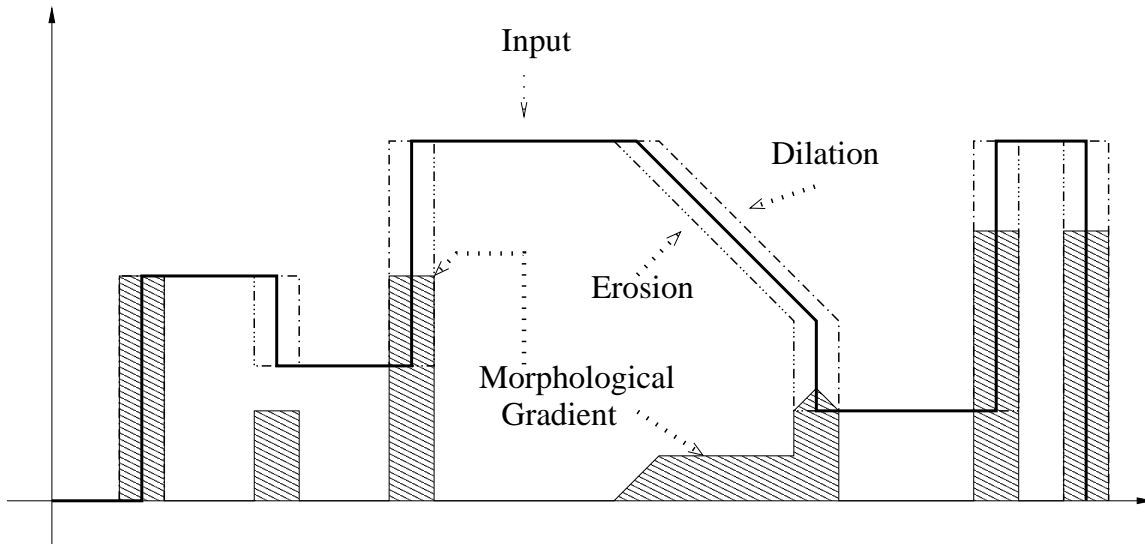


Figure 22: Illustration of morphological gradients on a 1-D profile.

8 Complex Watershed

The watershed transformation comes from an analogy between an image and a digital elevation model. A high intensity is analogous to a high altitude. Minima become lakes and maxima, mountains. Each ‘lake’ in an image drains an area called a catchment basin. These areas are separated by watersheds. The watershed transformation works by flooding the image through its minima until catchment basins collide. Such a collision occurs at the divides only. Whenever a collision occurs, a dam is erected to prevent mixing of water coming from different minima. At the end of the flooding process, only catchment basins separated by dams remain; the dams usually track the image crest-lines.

This transformation, used in conjunction with morphological gradients, constitute the basis of the morphological approach to segmentation [20] [14] [21] [15]. The morphological approach to the segmentation problem involves the use of markers. Markers located inside the object boundaries and markers that designate the background are created. It is assumed that between the shape and the background markers lies the edge that outline the object to be segmented.

Soille and Vincent [22] invented a fast algorithm that uses pixel queues. Meyer and Beucher modified it in two ways; first by flooding through markers only and second by using hierarchical queues [15] [23].

Regardless of the implementation, all these flooding simulations are based upon the order relationship in \mathbb{R} . Higher altitude pixels are flooded last. With the order

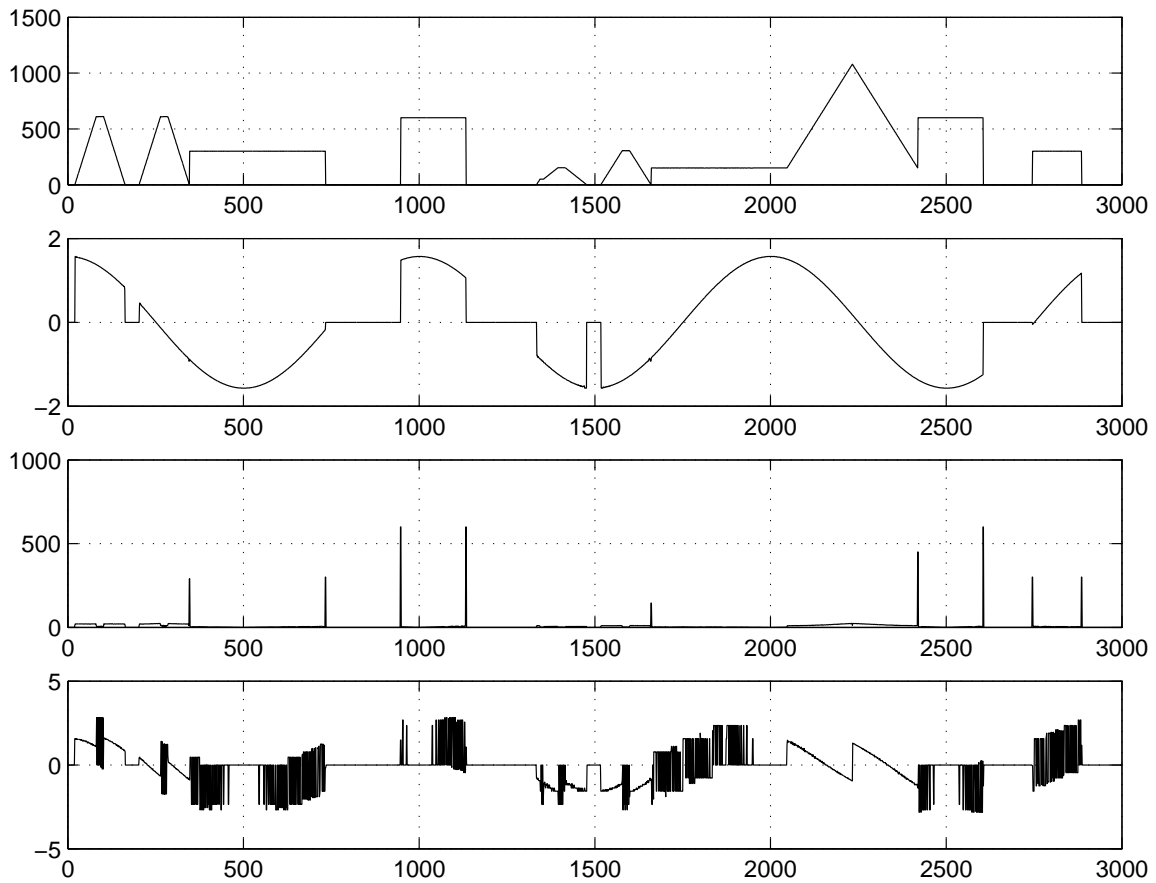


Figure 23: Beucher gradient on a complex signal. First two graphs: amplitude and phase in radians of the test signals. Last two graphs: amplitude and phase in radians of the Beucher Gradient.

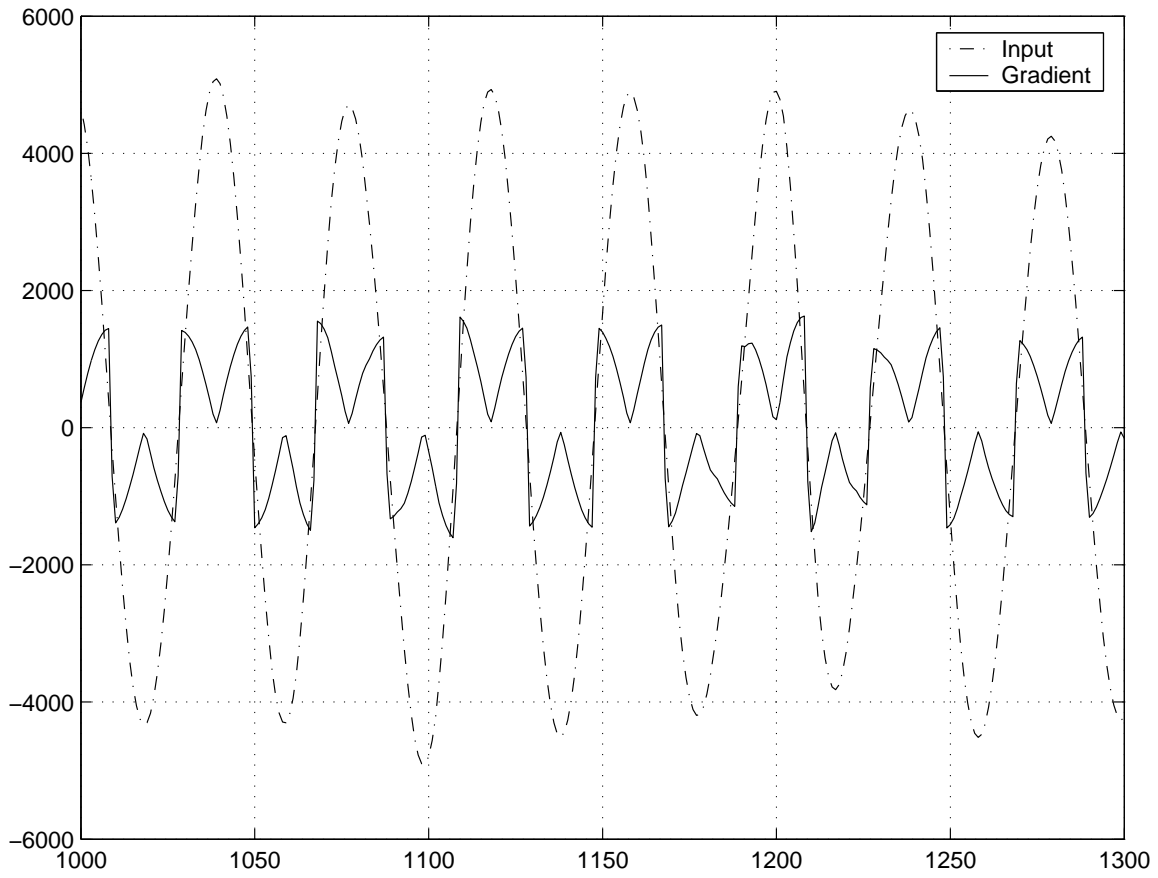


Figure 24: Complex Beucher gradient on a chirped (real) signal.

Space	$k = 0$	$k = 1$	$k = 2$	$k = 3$
Dimensions				
$n = 0$	Con. nbr.			
$n = 1$	Perim.	Con. nbr.		
$n = 2$	Area	Perim.	Con. nbr.	
$n = 3$	Volume	Area	Norm	Con. nbr.

Table 1: Minkowski functionals W_n^k where n is the space dimension and $k = 0, 1, \dots, n$. These are the volume, the area, the norm, the perimeter and the connectivity number.

relationship proposed in this report, one can say whether a complex pixel is “higher” than another one. Therefore, the extension of watershed algorithms through flooding simulations is done by a mere change of order relationships.

Fig. 25 shows an example of such a watershed, applied on a time-frequency representation of the chirped radar signal we used in other examples. The horizontal axis represents frequencies, while the vertical axis represents the time at which a windowed FFT has been computed on that signal. For the purpose of this illustration, we flooded the complex spectrogram using Meyer’s hierarchical queue. In order to generate the markers by which the complex image would be flooded, we assumed there would be only one frequency crest-line that was to be tracked over the spectrogram. This translates into the assumption there would be only two catchment basins separated by that crest-line. We therefore positioned the markers on both sides of the image and used the watershed to grow the catchment basins at the locations we knew the frequency peaks were not located, that is, at frequency 0 and at normalized frequency π .

The watershed transformation is therefore expanded with little difficulty to complex signals. The only modification needed was to change the order relationship used in the flooding simulations. All the present watershed algorithms use the usual order relationship on \mathbb{R} . They can all be expanded to complex signals through that modification.

9 Measurements

9.1 Basic Measurements and Minkowski Functionals

In morphology, measurements are done using Minkowski functionals, shown in Table 1. These measurements and their linear combinations, applied on a signal transformation, generates every possible measurement [4]. These are the volume, the area, the norm, the perimeter and the connectivity number.

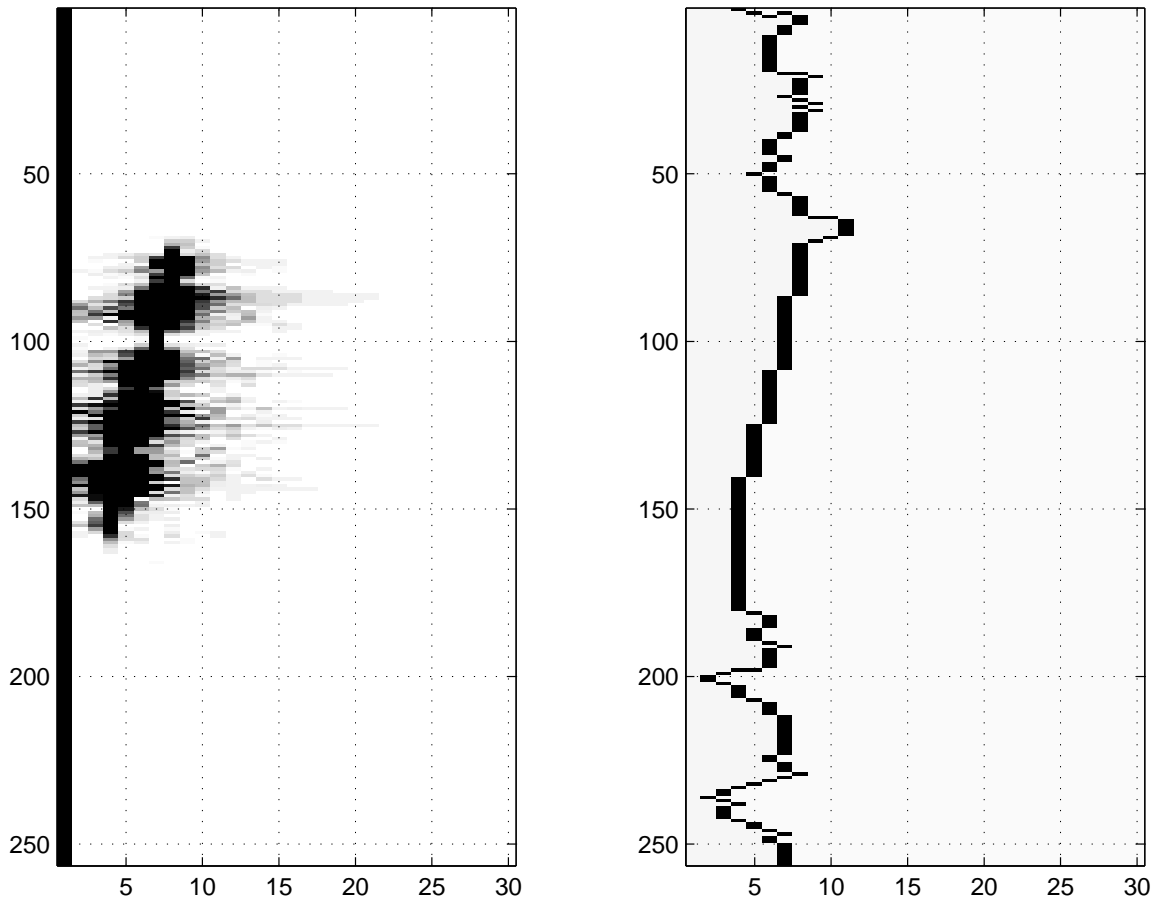


Figure 25: The complex watershed on a spectrogram. Left: the amplitude of the spectrogram, in gray scale. Right: the complex watershed of this spectrogram. The horizontal axis is the frequency while the vertical axis is the time. The units are arbitrary because it is a series of FFTs.

A complex signal is a 3-D object; it is described with three axes: the time, the real and the imaginary axes. In practice, the most important measure is the volume because it yields measurements that always have a physical signification. This is caused by the discrepancies between the physical units that describe signals; the time axis is expressed in seconds while the other axes are in Volts. The other functionals, with the exception of the Connectivity Number, do not preserve physical units [11].

With gray-tone images, the object from which a volume is measured is the gray-tone function and all the space below it; it is the umbra of the function. The umbra is dependent of the order relationship used. For complex signal samples, as shown in Fig. 2, it is a disk with its radius equal to the amplitude of the signal sample. Therefore, the umbra of a complex function $f(t)$ is the juxtaposition of the circular disks of radii $|f(t)|$. At time t , the area of the umbra is $\pi|f(t)|^2$. Therefore, the volume, or the Lebesgue Measure, $\mathcal{M}(f(t))$ of the umbra of the complex function $f(t)$ is the integral of all the superposed disks:

$$\mathcal{M}(f(t)) = \pi \int_{-\infty}^{\infty} |f(t)|^2 dt. \quad (48)$$

This measurement is also the energy of $f(t)$.

For RF signals in particular, the Lebesgue integral

$$\int_{-\infty}^{\infty} f(t) dt \quad (49)$$

tends to zero because there is usually no DC component in this type of signal. Although the average component of an image is an important feature, RF circuit designers strive to remove that component because it does not carry information and it is considered parasitic. This severely limits the usefulness of such a measurement because the DC component is in this case an artifact.

9.2 Granulometries and Pattern Spectra

Granulometry and Pattern Spectrum are two methodologies that are used with goals similar to spectral analysis. They allow to obtain size distributions of objects in pictures by using morphological openings and closings.

The granulometry and pattern spectrum proposed in this report share the same axiomatic basis as the classical granulometry. The tools were modified by using complex openings and closings instead of the usual openings; the Lebesgue measure was replaced by power measurements.

Granulometries are an axiomatization of the sieving process. One can obtain a size distribution of a powder by passing it through progressively finer sieves and by weighting the amount of powder that remains in each sieve. Matheron [24] formalized this process and discovered that a family of openings and closings of size λ was equivalent to a family of sieves. The Lebesgue measure is equivalent to the action of measuring masses. A granulometry of function f with a family of structuring elements B scaled by λ is then defined:

$$G(f, \lambda B) = \mathcal{M}(\gamma_{\lambda B}(f)), \quad (50)$$

where $\mathcal{M}(\gamma_{\lambda B}(f))$ is the Lebesgue measure of the opening of f with structuring element B scaled by a real, positive factor λ . The Lebesgue measure for binary images is the surface of objects. For gray-tone images, it is the volume and for functions, it is:

$$\mathcal{M}(f(t)) = \int_{-T/2}^{T/2} f(t) dt, \quad (51)$$

$T \rightarrow \infty$ being the length of the integration interval.

Maragos [25] defined the pattern spectrum as:

$$PS(f, \lambda B) = -\frac{d}{d\lambda} \mathcal{M}(\gamma_{\lambda B}(f)). \quad (52)$$

The pattern spectrum measures what was removed by the openings, that is, the objects that were trapped in the sieves. In contrast, the granulometry measures what passed through the sieves. The pattern spectrum actually measures the difference between successive openings. Maragos also defined the pattern spectrum for negative sizes using closings instead of openings:

$$PS(f, \lambda B) = \frac{d}{d\lambda} \mathcal{M}(\phi_{-\lambda B}(f)), \lambda < 0. \quad (53)$$

This is the equivalent of performing the pattern spectrum on the complement of an image, because the closing is the dual of the opening. There are granulometries based on closings instead of openings as well. These are also the same as computing a granulometry on the complement of an image.

9.3 Power Granulometry

Classical granulometries use the Lebesgue measure (Equation 49) to assess the amount of signal elements that survived the openings. RF signals are usually symmetrical with respect to the time axis, unless there is an undesirable DC component added to them. Complex morphological operators tend to preserve such symmetry. Consequently, the Lebesgue measure tends to zero for such signals. As λ increases, any deviation of the Lebesgue measure from zero is likely caused by artifacts such as border and sampling effects. This situation is corrected by replacing the Lebesgue measure with the signal power. The power granulometry is then defined:

$$G^P(f, \lambda B) = \frac{1}{T} \int_{-T/2}^{T/2} \gamma_{\lambda B}^C(f(t)) \gamma_{\lambda B}^C(f(t))^* dt = \frac{1}{T} \int_{-T/2}^{T/2} |\gamma_{\lambda B}^C(f(t))|^2 dt, \quad (54)$$

where $\gamma_{\lambda B}^C(f(t))$ is the complex opening with structuring element B scaled by a factor λ . $\gamma_{\lambda B}^C(f(t))^*$ is the complex conjugate of $\gamma_{\lambda B}^C(f(t))$.

Performing the Lebesgue measure on the difference between successive openings is the same as performing the derivative of the Lebesgue measure over successive openings:

$$\lim_{\Delta \rightarrow 0} \frac{1}{\Delta} [\mathcal{M}(\gamma_{\lambda B}(f(t)) - \gamma_{(\lambda+\Delta)B}(f(t)))] = -\frac{d}{d\lambda} \mathcal{M}(\gamma_{(\lambda)B}(f(t))). \quad (55)$$

It is no longer the case for nonlinear measurements such as power. Therefore, it is no longer possible to use the current definition of pattern spectrum in Eq. 52. It is preferable to compute the power of the residues between the successive openings. This yields the following definition for the power pattern spectrum:

$$PS^P(f, \lambda B) = \lim_{\Delta \rightarrow 0} \frac{1}{\Delta T} \int_{-T/2}^{T/2} |\gamma_{\lambda B}^C(f(t)) - \gamma_{(\lambda+\Delta)B}^C(f(t))|^2 dt, \lambda \geq 0. \quad (56)$$

Following Maragos, the power pattern spectrum for negative sizes is:

$$PS^P(f, \lambda B) = \lim_{\Delta \rightarrow 0} \frac{1}{\Delta T} \int_{-T/2}^{T/2} |\phi_{(-\lambda+\Delta)B}^C(f(t)) - \phi_{-\lambda B}^C(f(t))|^2 dt, \lambda \leq 0. \quad (57)$$

$\phi^C()$ is the complex closing.

9.3.1 Examples

In order to illustrate these concepts, the following signals have been used:

1. A simulated fixed frequency radar pulse. The period of the sinusoid was 50 samples.
2. Another simulated fixed frequency radar pulse. The period of the sinusoid was 25 samples.
3. A simulated signal composed of two tones. The period of the first tone was 50 samples and it was 25 for the second tone.
4. A real chirped radar signal, with the period of the carrier starting at 50 samples and ending at 85 samples.

These signals were analyzed with a power granulometry and a power pattern spectrum with a flat structuring element of diameter $\lambda = \{3, 5, 7 \dots 41\}$.

Fig. 26 shows the simulated pulse with a period of 50 samples. The signal instantaneous power is periodic with a 25-sample period. Fig. 27 shows the resulting power granulometry and power pattern spectrum. The main feature of the power pattern spectrum is its peak at 25 samples. This corresponds well with the period of the instantaneous power fluctuations present in the signal. The rate of growth of this peak increases with λ . This reflects the shape of the sinusoid; the structuring element progressively brings the signal amplitude down to zero, which is where the power fluctuations are the largest.

Fig. 28 shows the power granulometry and pattern spectrum of the simulated pulse featuring a carrier period of 25 samples. The granulometry and the pattern spectrum scaled by a factor two along the λ axis. The peak in the pattern spectrum has moved to a period of 13 samples. The remaining peak, at $\lambda = 25$ samples, was caused by sampling artifacts.

Fig. 30 shows the measurements of a two-tone signal. It should be noted that even though this signal is the result of the linear combination of two signals, this is not visible in the pattern spectrum. This is to be expected, because the pattern spectrum shows the shapes in the time domain instead of the frequency domain. The successive peaks can be observed in Fig. 29, which details a section of the pulse. These peaks and valleys do indeed exhibit the various sizes shown on the pattern spectrum.

Fig. 31 shows the measurements of a chirped radar signal. The difference with the other signals is striking. The chirped radar features wider peaks because the size of the instantaneous power variations vary more widely than in the case of the simulated signals.

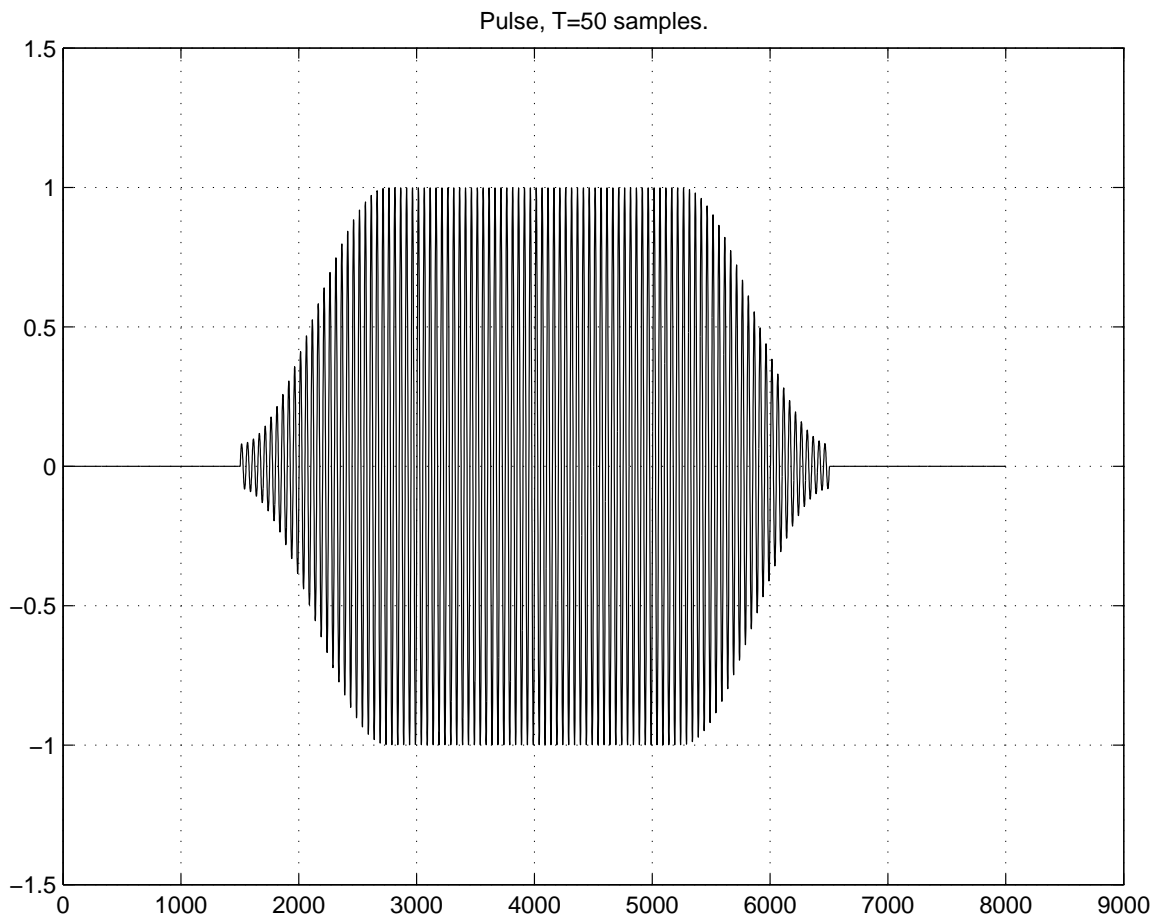


Figure 26: Simulated radar pulse. Period = 50 samples.

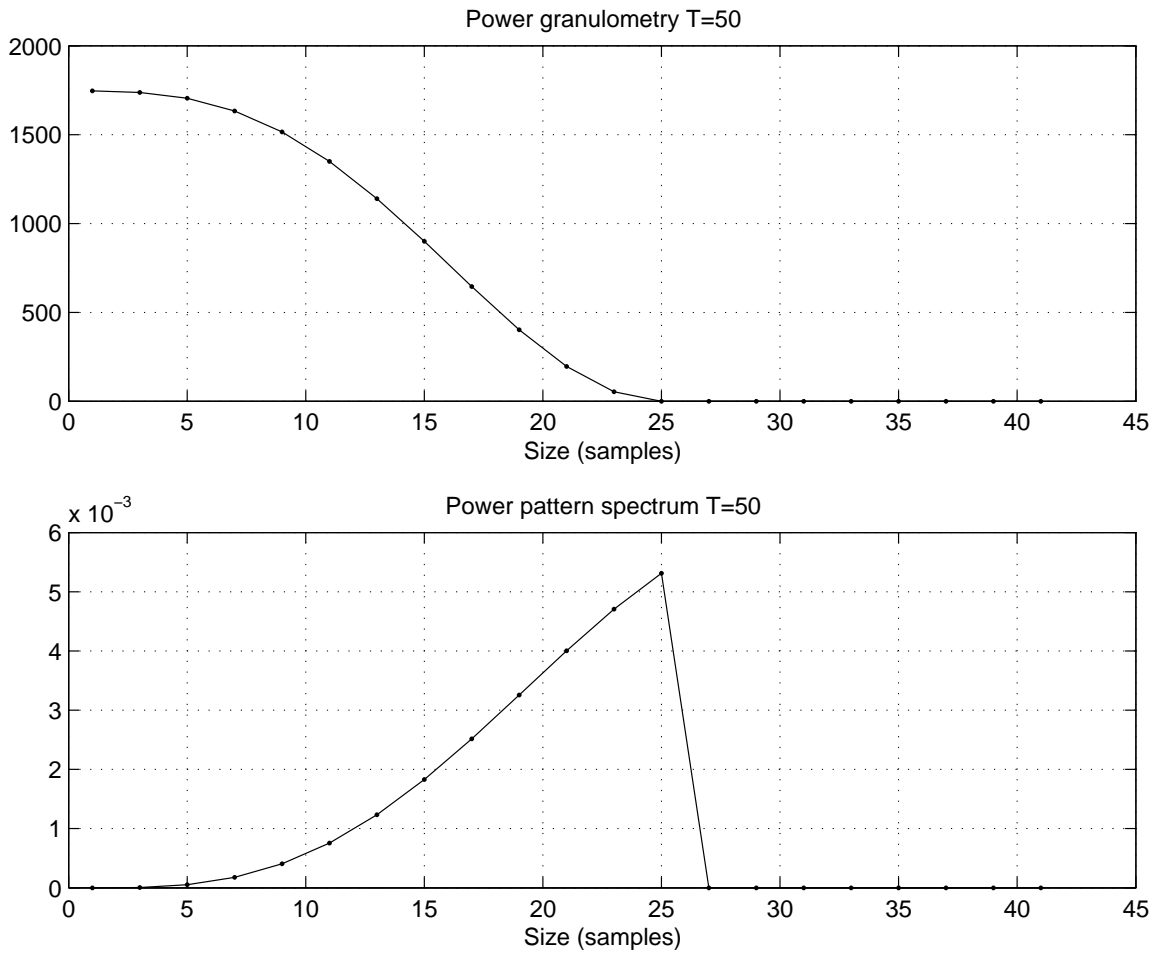


Figure 27: Power granulometry and power pattern spectrum of a simulated pulse. Period = 50 samples.

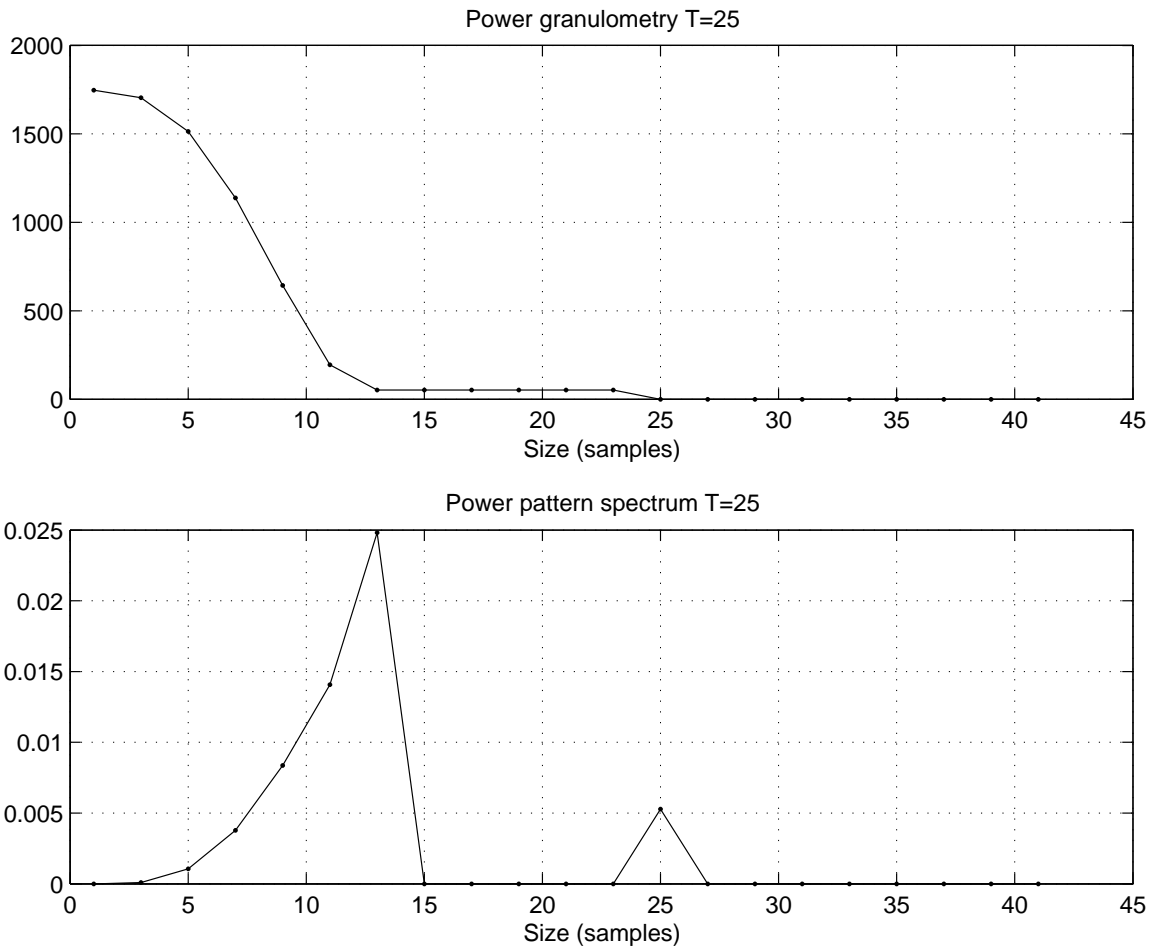


Figure 28: Power granulometry and power pattern spectrum of a simulated pulse. Period = 25 samples.

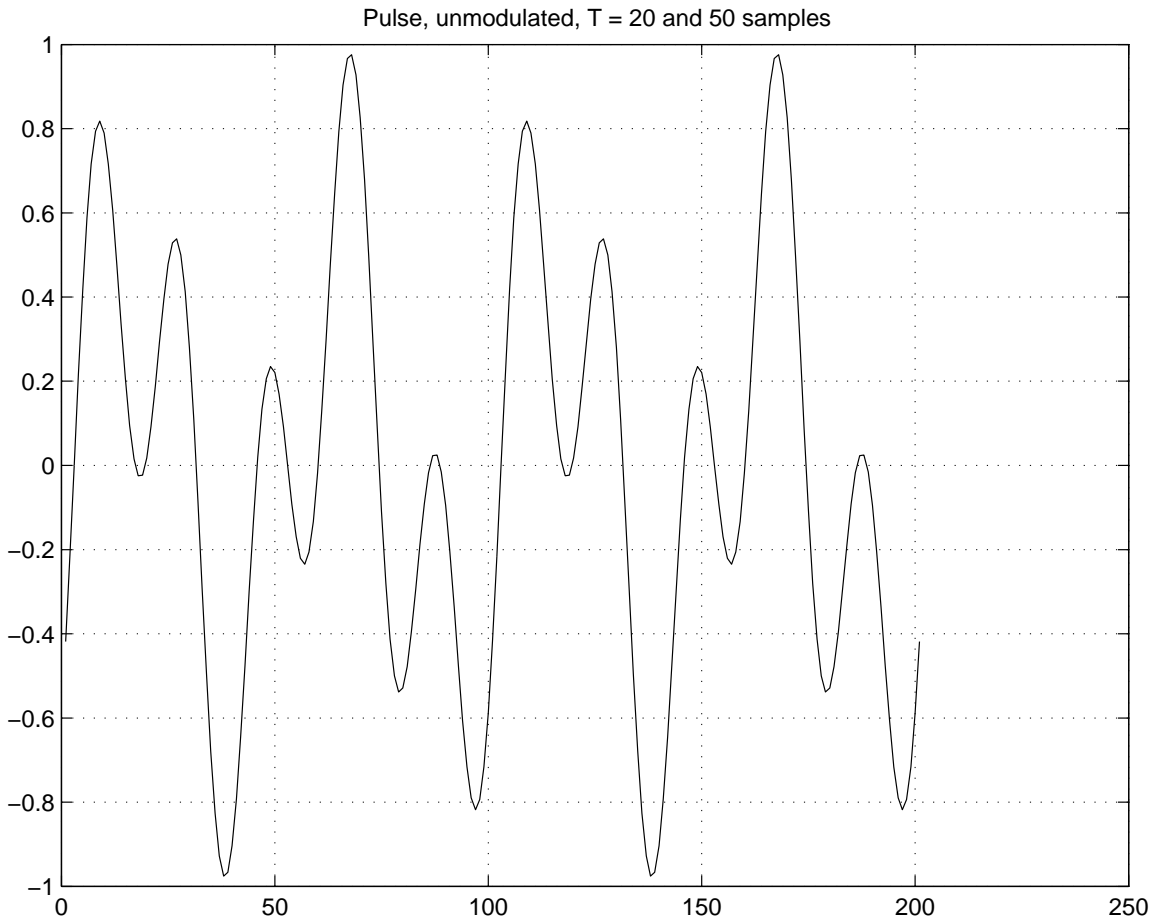


Figure 29: Pulse fragment, superposition of two tones (Period: 20 and 50 samples).

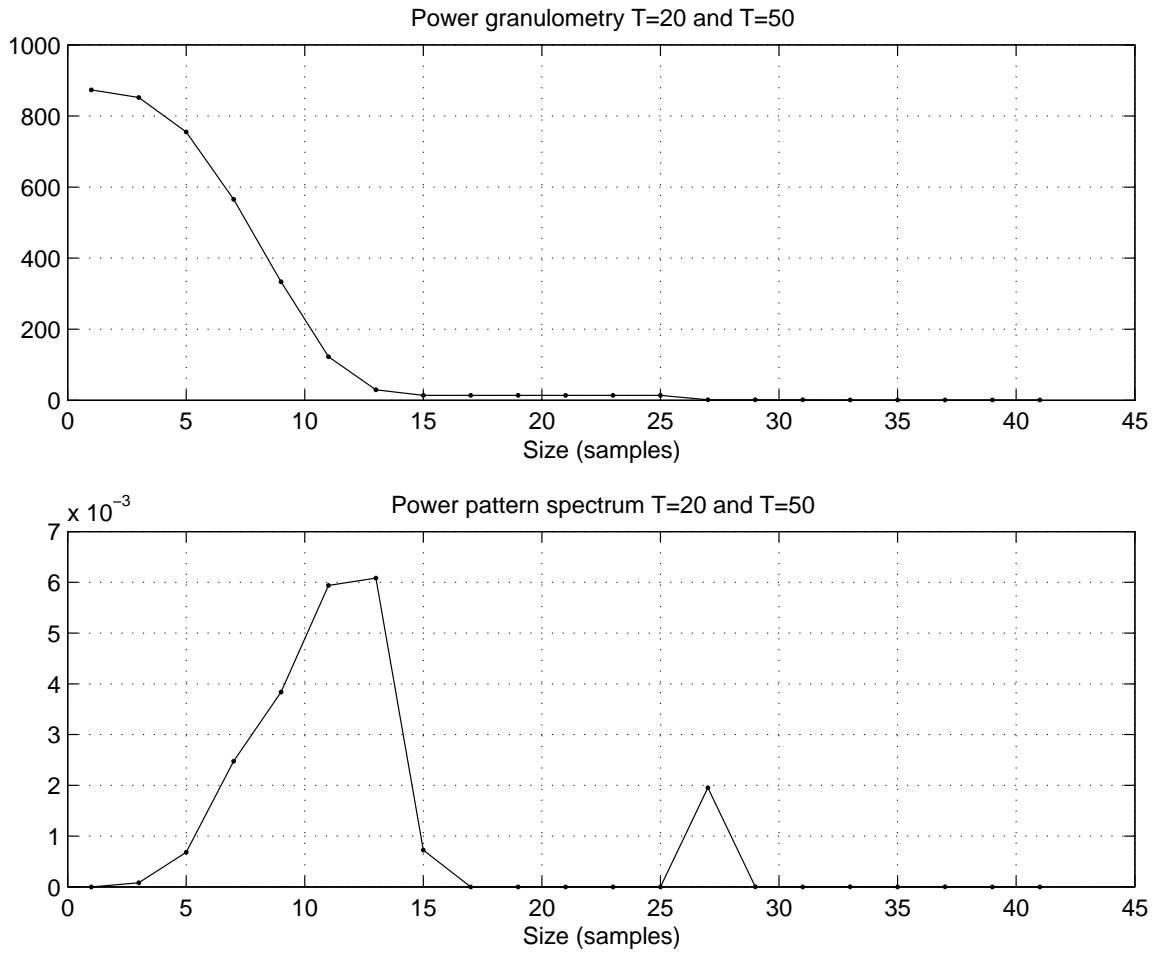


Figure 30: Power granulometry and power pattern spectrum of a simulated pulse. Superposition of two tones (Period: 20 and 50 samples).

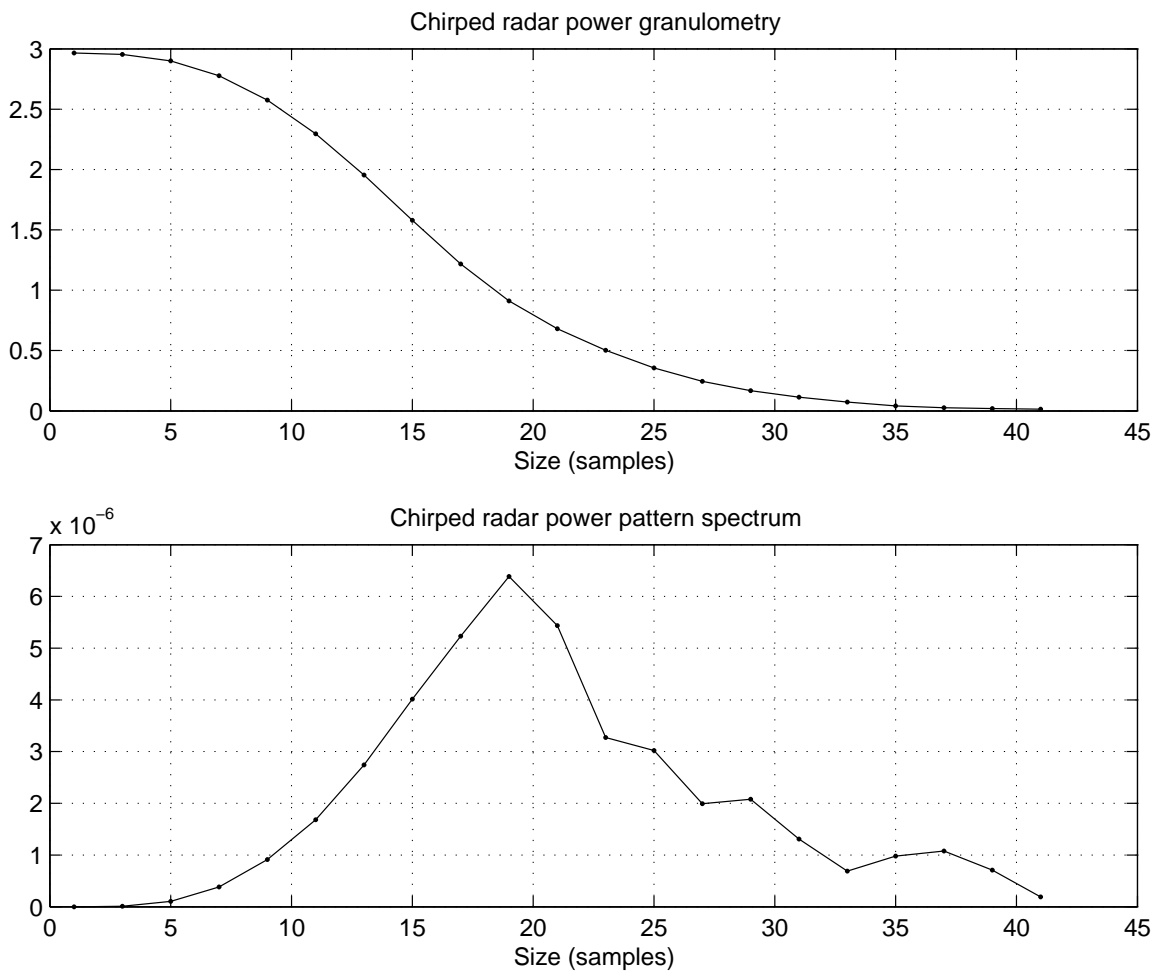


Figure 31: Power granulometry and power pattern spectrum of a chirped radar pulse.

This section presented a new type of granulometry and pattern spectrum. These are more appropriate to the context of complex signal processing than the classical granulometry and pattern spectrum for the following reasons: first, complex signals are often represented using complex functions and second, these signals are compared using their amplitude and power instead of the value of the signals themselves.

The granulometry was modified in two ways. The Lebesgue integral was substituted with the power measurement. The morphological opening was also replaced with a complex opening. It turned out that this complex opening was more appropriate for purely real signals than the classical opening.

The definition of pattern spectrum was also modified. Instead of computing the first derivative of the granulometric curve relative to the structuring element size λ , the power measurement on the difference between adjacent openings was computed.

Granulometries and pattern spectra perform time-domain measurements of objects embedded in signals. The transformations used to obtain these measurements are nonlinear; therefore, the concept of linear superposition is not valid in this context. Two sinusoids cannot be separated in this fashion; the superposition of two pattern spectra does not directly correspond to the pattern spectrum of the two signals that featured these spectra. Granulometries and pattern spectra have similar goals to spectral analysis; yet they are complementary to this methodology.

10 Implementation Notes

It is possible to re-use classical implementations of morphological operators. This is what has been done in the examples we presented in this report.

The procedure involves converting the complex signal samples into unambiguous scalars. This is done by creating a table that contains all the complex samples. All the samples are sorted using the total order relationship we proposed in this report. Then, redundant samples, that is, samples that are identical are removed. Then, an index is assigned to every non-redundant sample. Finally, a new signal or image is created by replacing all the complex samples with their corresponding indexes. Morphological operators are then applied and the conversion from the new index signal or picture to the resulting complex signal is carried out.

This is possible because morphological operators do not create new complex values. The maximum(\vee)/minimum(\wedge) operators simply select among complex samples. One must be however cautious when mixing arithmetic and morphological operators because these operations do create complex values that did not exist in the input images.

By so doing, all the already implemented operators and transforms can be re-used in an elegant and simple manner. It is even possible to use already implemented special hardware processors with no other modification than the index conversion front-end.

11 Conclusion

In this report, we expanded Mathematical Morphology to complex signals. This expansion was carried out by changing the order relationship used to compare two signal samples. Although there is no natural way to create an order relationship between multivariate data such as complex numbers, we create such a relationship. This order relationship is a total order relationship – the same as the one that orders gray-tone pixels. It is also compatible with the practice of RF and complex signal processing, for which energy and power considerations are of a fundamental importance. It therefore has physical significance. Moreover, the relationship gracefully degenerates into the same order relationship used in gray-tone morphology when complex signals become real and positive. Yet, there is an inevitable degree of arbitrariness in this order relationship. For instance, one might argue that the lexicographic ordering used when two samples feature the same amplitude should be reversed, therefore giving priority to the imaginary part instead of the real part as we suggested in this report. Indeed, there is no reason to prefer one over the other; a choice must be made.

A new complementation procedure was also invented because of the new order relationship. The usual gray-tone complement was not applicable to that class of signals. For instance, the negation, which is used on \mathbb{R}^n , does not reverse our order relationship. In the same way as the new order relationship, the complementation also degenerates into the usual gray-tone complement when the complex signals become real and positive.

Because of this new total order relationship and this new complementation procedure, all the mathematical results that are applicable to gray-tone morphology are also applicable to complex signals. Fundamental properties like extensivity and anti-extensivity have to be assessed through the new order relationship. Duality is achieved by using the complex complement.

In this report, we created the basic morphological operators using the new order relationship. We then carried on by presenting examples of complex openings and closings. Geodesic transformations were then presented. The extension of the classical transformation to complex transformations was straightforward, with the exception of the complex regional minima and maxima detectors in Section 5.5. The additions and subtraction by constants were replaced by multiplications because this is more compatible with the order relationship.

The shape of the umbra of a complex function is radically different from the shape of a gray-tone function. Therefore, the implementation of the Lebesgue measure was changed in this report. It turned out this measure is the same as the energy of the complex signal under analysis, normalized by a constant. This result is important because it connects with the current practice of making energy and power measurements on a signal.

In this research, we also discovered that this new Mathematical Morphology was also useful in processing real signals. It turns out that this kind of morphology is more appropriate to AC signals, that is, signals that are not characterized by their DC component, such as audio, ultrasound or RF signals. Classical Mathematical Morphology does not perform well on those signals because it tends to create undesirable artifacts such as increasing the energy of the output and creating artificial DC components.

This extension of Mathematical Morphology enables us now to apply it to the following examples:

- Complex signals, such as communication and radar signals that feature an in-phase and an in-quadrature component.
- Fourier transforms.
- Spectrograms and other time-frequency representations.

At the present time, RF signals are best understood using linear methods such as the Fourier transform and convolutions. This is perfectly justifiable; after all, RF signals propagate through linear media. However, non-linearities do exist in most RF systems by design. When non-linearities are accidental, Fourier analysis usually breaks down. Harmonics and intermodulation distortion make the spectrum of the signal unrecognizable. When non-linearities exist by design, using linear tools to analyze and model the RF system is difficult. These non-linearities are frequent: they exist whenever modulation is used and they exist in pattern recognition systems whenever information is irreversibly destroyed.

Morphological tools show some promise in filtering, pattern recognition and feature extraction of radar signals. Granulometries can be used with similar goals as those of Fourier analysis. This report was mainly oriented towards features extraction in radar signals. This is also one of the applications of Fourier analysis. Another application of the frequency representation of signals is the modelling of linear operators. Granulometries, by obtaining the size distribution of a signal, can also model the spatial component of non-linear transformations.

References

- [1] Serra, J. (1987), Morphological optics, *Journal of Microscopy*, 145(Pt1), 1–22.
- [2] Marr, D. (1976), Early Processing of Visual Information, *Phil. Trans. Royal Soc. London*, B 275(942), 483–524.
- [3] Barnett, V. (1976), The Ordering of Multivariate Data, *J. R. Statist. Soc. A*, 139(Part 3), 318–355.
- [4] Serra, J. (1982), Image analysis and mathematical morphology, London: Academic Press.
- [5] Comer, M.L. and Delp, E.J. (1992), An empirical study of morphological operators in color image enhancement, In SPIE, (Ed.), *Proceedings SPIE, Image Processing Algorithms and Techniques III*, Vol. 1657, pp. 314–325.
- [6] Comer, M.L. and Delp, E.J. (1999), Morphological Operations For Color Image Processing, *Journal of Electronic Imaging*, 8(3), 279–289.
- [7] Astola, J., Haavisto, P., and Neuvo, Y. (1990), Vector median Filters, *Proceedings of the IEEE*, 78(4), 678–689.
- [8] Talbot, H., Evans, C., and Jones, R. (1998), Complete Ordering and Multivariate Mathematical Morphology, In Heijmans, H. and Roerdink, J., (Eds.), *Mathematical Morphology and Its Applications to Image and Signal Processing*, pp. 27–34, Amsterdam: Kluwer Academic Press.
- [9] Chanussot, J. and Lambert, P. (1998), Total Ordering Based on Space Filling Curves For Multivalued Morphology, In Heijmans, H. and Roerdink, J., (Eds.), *Mathematical Morphology and Its Applications to Image and Signal Processing*, pp. 51–58, Amsterdam: Kluwer Academic Press.
- [10] Rivest, J.-F. (2004), Morphological operators on complex signals, *Signal Processing*, 84, 133–139.
- [11] Rivest, J.-F., Serra, J., and Soille, P. (1992), Dimensionality in image analysis, *Journal of Visual Communication and Image Representation*, 3(2), 137–146.
- [12] Serra, Jean (1988), Introduction to Morphological Filters, Ch. 5, pp. 101–114, London: Academic Press.
- [13] Lantuéjoul, C. and Beucher, S. (1981), On the Use of Geodesic Metric in Image Analysis, *Journal of Microscopy*, 121, 39–49.

- [14] Beucher, S. (1990), Segmentation d'images et morphologie mathématique, Ph.D. thesis, Ecole des Mines de Paris.
- [15] Meyer, Fernand and Beucher, S. (1990), Morphological Segmentation, *Journal of Visual Communication and Image Representation*, 1(1), 21–46.
- [16] Vincent, L. (1993), Morphological grayscale reconstruction in image analysis: applications and efficient algorithms, *IEEE Transactions on Image Processing*, 2(2), 176–201.
- [17] Vincent, Luc (1990), Algorithmes morphologiques à base de files d'attente et de lacets. Extension aux graphes, Ph.D. thesis, Ecole des Mines de Paris.
- [18] Meyer, F. (1979), Cytologie quantitative et morphologie mathématique, Ph.D. thesis, Ecole des Mines de Paris.
- [19] Rivest, J.F., Soille, P., and Beucher, S. (1993), Morphological Gradients, *Journal of Electronic Imaging*, 2(4), 326–336.
- [20] Beucher, S. and Lantuéjoul, C. (1979), Use of Watersheds in Contour Detection, In *International Workshop on Image Processing: Real-Time Edge and Motion detection/estimation*, Rennes, CCETT/IRISA.
- [21] Beucher, S. (1982), Watersheds of functions and picture segmentation, In *IEEE Int. Conf. on Acoustics, Speech and Signal Processing*, pp. 1928–1931, Paris.
- [22] Vincent, Luc and Soille, Pierre (1991), Watersheds in Digital Spaces: An Efficient Algorithm Based on Immersion simulations, *IEEE Transactions on Pattern Analysis and Machine Intelligence*, 13(6), 583–598.
- [23] Meyer, Fernand (1990), Algorithmes ordonnés de ligne de partage des eaux, (Technical Report N-06/90/MM), Centre de Morphologie Mathématique Ecole des Mines de Paris.
- [24] Matheron, G. (1975), *Random Sets and Integral Geometry*, New York: John Wiley & Sons.
- [25] Maragos, P. (1989), Pattern Spectrum and Multiscale Shape Representation, *IEEE Trans. Pattern Anal. Mach. Intell.*, 11(7), 701–716.

This page intentionally left blank.

DOCUMENT CONTROL DATA

(Security classification of title, body of abstract and indexing annotation must be entered when document is classified)

1. ORIGINATOR (the name and address of the organization preparing the document. Organizations for whom the document was prepared, e.g. Centre sponsoring a contractor's report, or tasking agency, are entered in section 8.) Defence R&D Canada – Ottawa 3701 Carling, Ottawa, ON, Canada K1A 0Z4		2. SECURITY CLASSIFICATION (overall security classification of the document including special warning terms if applicable). UNCLASSIFIED	
3. TITLE (the complete document title as indicated on the title page. Its classification should be indicated by the appropriate abbreviation (S,C,R or U) in parentheses after the title). Morphological Processing of Complex Signals			
4. AUTHORS (last name, first name, middle initial) Rivest, Jean-F.			
5. DATE OF PUBLICATION (month and year of publication of document) January 2006	6a. NO. OF PAGES (total containing information. Include Annexes, Appendices, etc). 76	6b. NO. OF REFS (total cited in document) 25	
7. DESCRIPTIVE NOTES (the category of the document, e.g. technical report, technical note or memorandum. If appropriate, enter the type of report, e.g. interim, progress, summary, annual or final. Give the inclusive dates when a specific reporting period is covered). Technical Report			
8. SPONSORING ACTIVITY (the name of the department project office or laboratory sponsoring the research and development. Include address). Defence R&D Canada – Ottawa 3701 Carling, Ottawa, ON, Canada K1A 0Z4			
9a. PROJECT NO. (the applicable research and development project number under which the document was written. Specify whether project). 13en	9b. GRANT OR CONTRACT NO. (if appropriate, the applicable number under which the document was written).		
10a. ORIGINATOR'S DOCUMENT NUMBER (the official document number by which the document is identified by the originating activity. This number must be unique.) DRDC Ottawa TR 2006-004	10b. OTHER DOCUMENT NOS. (Any other numbers which may be assigned this document either by the originator or by the sponsor.)		
11. DOCUMENT AVAILABILITY (any limitations on further dissemination of the document, other than those imposed by security classification) (X) Unlimited distribution () Defence departments and defence contractors; further distribution only as approved () Defence departments and Canadian defence contractors; further distribution only as approved () Government departments and agencies; further distribution only as approved () Defence departments; further distribution only as approved () Other (please specify):			
12. DOCUMENT ANNOUNCEMENT (any limitation to the bibliographic announcement of this document. This will normally correspond to the Document Availability (11). However, where further distribution beyond the audience specified in (11) is possible, a wider announcement audience may be selected). Unlimited.			

13. ABSTRACT (a brief and factual summary of the document. It may also appear elsewhere in the body of the document itself. It is highly desirable that the abstract of classified documents be unclassified. Each paragraph of the abstract shall begin with an indication of the security classification of the information in the paragraph (unless the document itself is unclassified) represented as (S), (C), (R), or (U). It is not necessary to include here abstracts in both official languages unless the text is bilingual).

This report presents an extension of Mathematical Morphology to complex signals. This extension is done by modifying the order relationship upon which all the morphological operators are based. This extension of Mathematical Morphology is essential if one wishes to use the methods of MM to process complex signals, such as communication and radar signals that feature an in-phase and an in-quadrature component.

All the basic operators such as dilations, erosions, openings and closings are developed in this report. The concept of geodesy on complex signals is explored in detail, along with the morphological approach to segmentation. The complex watershed transformation is also developed. These transformations are illustrated on complex test signals, radar signals, Fast Fourier Transforms and complex spectrograms.

Because of the proposed order relationship, the umbra of a complex signal is radically different from the umbra of a gray-tone function. Therefore, the implementation of measurements is also different from the classical measurements performed on gray-tone images. This is illustrated with an example: granulometry and pattern spectrum on a chirped radar signal.

14. KEYWORDS, DESCRIPTORS or IDENTIFIERS (technically meaningful terms or short phrases that characterize a document and could be helpful in cataloguing the document. They should be selected so that no security classification is required. Identifiers, such as equipment model designation, trade name, military project code name, geographic location may also be included. If possible keywords should be selected from a published thesaurus. e.g. Thesaurus of Engineering and Scientific Terms (TEST) and that thesaurus-identified. If it not possible to select indexing terms which are Unclassified, the classification of each should be indicated as with the title).

Mathematical Morphology
Signal Processing
Electronic Support

Defence R&D Canada

Canada's leader in Defence
and National Security
Science and Technology

R & D pour la défense Canada

Chef de file au Canada en matière
de science et de technologie pour
la défense et la sécurité nationale



www.drdc-rddc.gc.ca